Exploration of microwave-assisted breakage of rocks:

The effect of size, shape, and internal discontinuity of rock on microwave distribution

By

Fan Liu

November 2014

Department of Mining &Materials Engineering

McGill University

Montreal, Quebec, Canada

A thesis submitted to McGill University

In partial fulfillment of the requirements for the degree of

Master of Engineering

Abstract

Microwave- assisted breakage of rocks has proved to be more efficient than traditional methods at separating valuable minerals from gangue during mineral processing. However, little research has been conducted in terms of the applications of microwave-assisted rock breakage to tunnel excavation. The combination of a microwave system and Tunnel Boring Machine (TBM) has the potential to be an efficient tunnel excavation tool that is suitable in operating in both hard and soft rock conditions. As a small component of a larger project related to the microwave-assisted TBMs, the purpose of this thesis is to experimentally demonstrate internal temperature distribution properties for basalt rocks having different sizes, shapes, and internal spacing. In addition, correlations are quantified among microwave absorption, volume, and sample temperature after microwave treatment in a multimode cavity.

Key finding are:

1. When the diameter to height ratio of a cylindrical core is more than 1, only one peak temperature appears somewhere in the middle of the core. When the ratio is less than 1, two temperature peaks appear near the ends of the core, and the diameter to height ratio that can result in two temperature peaks increases as the diameter of the core increases;
2. The shape has no obvious influence on temperature distribution;
3. Internal spacing of 1mm doesn't influence the temperature distribution when the core is fully exposed to microwave radiation. Internal spacing of more than 1mm significantly reduces heating efficiency when only one surface of the core is exposed to plane microwave radiation;
4. The electromagnetic power absorption increases and the average temperature decreases with increasing sample volume. The trends are well described by power series.

Acknowledgement

I would like to express my sincere gratitude to my supervisor, Prof. Ferri Hassani, for his constant support and guidance in both financial and academic aspects throughout the course of this project. I would also like to thank Dr. Pejman Nekoovaght for his generous help and great patience that are indispensible in finishing this project

Table of contents

Nomenclature

E: Electrical field intensity in general

E_0: **Electric field intensity determined by source**

E_{max}: **Peak electric field intensity**

E_1^+: **Electric field intensity of incident wave in medium 1**

E_1^-: **Electric field intensity of reflected wave in medium 1**

E_2^+: **Transmitted wave in medium 2**

H: **Magnetic field intensity**

H^*: **Conjugate of a complex magnetic field**

ε_0: **Permittivity of free space**

μ_0: **Permeability of free space**

ε_r: **Relative permittivity of dielectric**

μ_r: **Relative permeability of dielectric**

ε''_{eff}: **Effective loss factor of a dielectric**

ε': **Dielectric constant a dielectric**

j: Indicator of imaginary part

$\frac{\partial}{\partial t}$: **Derivation with respect to time**

J: **Electric current density**

∇: **Del operator**

$\times$: **Cross product (curl)**

$\cdot$: **Dot product (divergence)**

ρ_e: **Electric charge density**

ρ_b: **Density of basalt**

B: **Magnetic flux**

ω: **Angular frequency**

β: **Propagation constant along z direction**

α: **Attenuation coefficient**

z: **Displacement in z direction**

v: **Speed of electromagnetic wave**

λ: **Wave length**

P: **Average electromagnetic power density over time**

$P_{surface}$: **Average power absorbed by a surface**

P_{trans}: **Transmitted power**

P_{final}: **Power left after penetration**

T: **Final temperature**

T_0: **Initial temperature**

t: **Time**

V: **Volume**

Q: **Heat energy**

$E_{rms} = \frac{E_{max}}{\sqrt{2}}$: **Rms value of electric field peak intensity**

Re: **Real part of a complex number**

Im: **Imaginary part of a complex number**

D_p: **Penetration depth**

m, n, l: **Mode number of electromagnetic wave inside a cavity**

a, b, c:	**Dimensions of a cavity**
η **:**	**Impedance of a dielectric**
Γ:	**Reflection coefficient**
$\boldsymbol{k}$:	**Propagation constant in general direction**
C:	**Specific heat**
A:	**Surface area**
d:	**Thickness**
$\boldsymbol{T_{hot}}$**:**	**Hotter area of an object**
$\boldsymbol{T_{cold}}$**:**	**Colder area of an object**

List of Figures

List of Tables

I. Introduction

1.1. A novel technology for rock breakage

“If agriculture is mankind's most important endeavor in the earliest civilization, mining probably ranked second. These two industries have been vital to the existence of human beings since the beginning of civilization” (**Madigan, 1981**). This statement demonstrates the importance of mining in revolutionizing ancient society, as one of the activities that ran in parallel with human civilization. At that time, mechanical force was the only way human were able to apply to break rocks, which was very time consuming yet had very little effects (**Coulson, 2012**). During the New Stone age, human learned the technique of using fire ignited with flint to heat rock and quench them with cold water afterwards **(Hartman, 1992)**; the process of expansion and contraction reduced strength so it becomes easier to break.

This traditional rock mass breakage technique involving the use of thermal energy is still applicable, at the expense of tremendous energy waste in the conduction and convection processes, and with limited overall results. However, the thermal energy produced by microwaves has shown to be a much more efficient and less energy costly method to treat most rocks (**Jones et al., 2004**). The extremely fast oscillation of the electromagnetic field can induce microscopic activities such as dipole oscillation, rotation, and ion migration (**Metaxas and Meredith, 1983**), by which an enormous amount of heat can be generated within the rocks. The heat generated from the interior of the rock mass spreads out to the surface, a process that creates mechanical stresses. When these stresses exceed the fracture stress for most rocks, micro cracks form in the rocks, which then lead to significant emolliating of their structure (**Prokopenko, 2011**).

Microwave assisted mineral processing to separate valuable minerals from gangues has been studied since the mid-1980s; some applications were very successful in a variety of mineral processing fields. (**Kingman et al., 2000, 2004; Napier-Munn and Wills, 2006; McGill et.al., 1988; Walkiewicz, 2002; Standish and Huang, 1991; Huang and Rowson, 2002; Wang and Forssberg, 2003; Koleini and Barani, 2012)** However, microwave assisted tunnel excavation, which could be another possible promising technology has not been well evaluated and studied.

1.2. The prototype of microwave -assisted Tunnel Boring Machine (TBM)

Currently and as an alternative to the time-consuming conventional blasting and drilling method that relies on powders, explosives and other excavation machineries to dig tunnels(**HAPGOOD,2004**), TBMs are often used for heavy tunnel excavations. A TBM can bore through anything from hard rock to sand and is not limited by surrounding ground. It creates cracks on the tunnel wall by biting into it through disc cutters located on the cutter head (Figure 1-1). Both the cutter head and discs rotate at the same time while the machine is advancing to create force in different directions that can “tear” the wall.

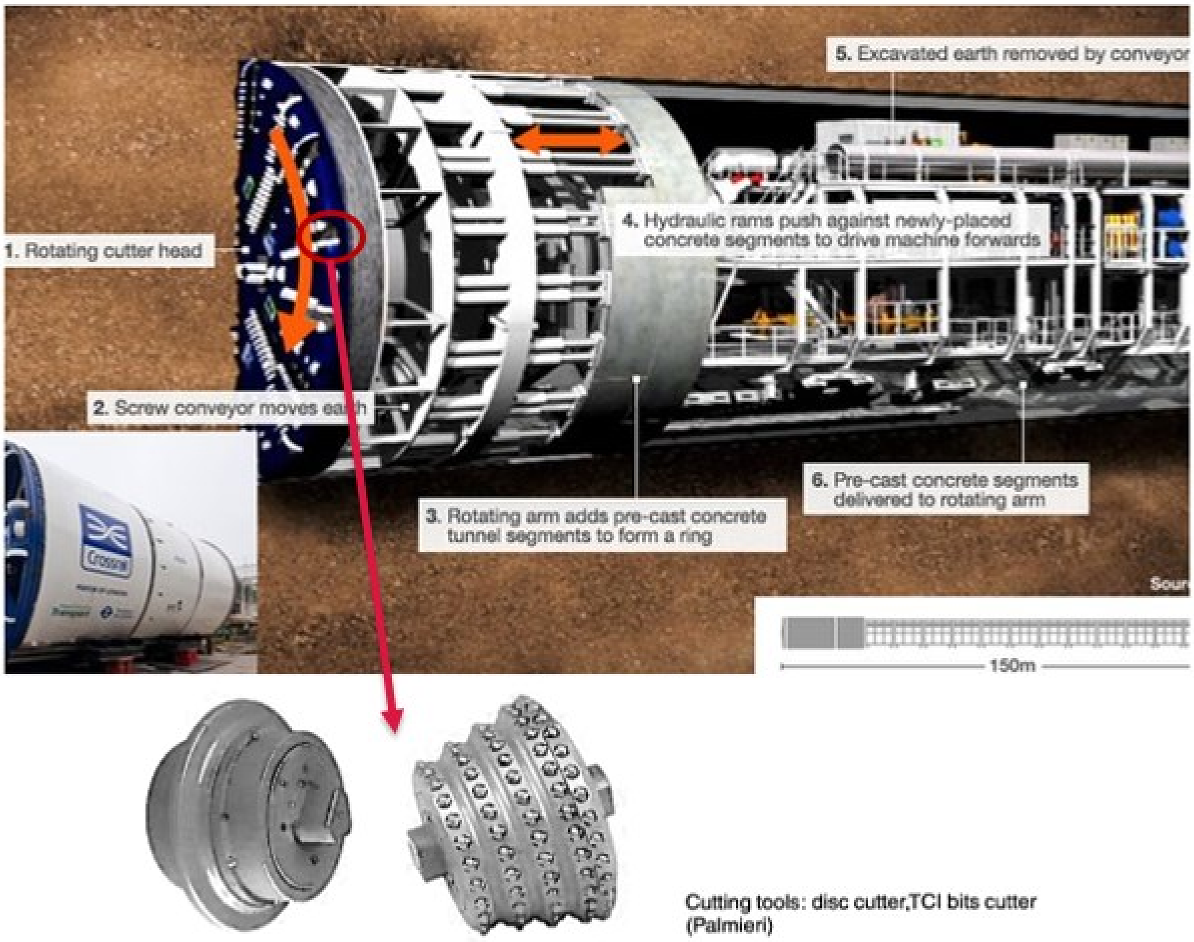

Figure 1-1. Disc cutters used to create cracks on the tunnel wall (Maidl et al., 2008)

As the demand for communication and transportation increases, TBMs are developed to be more tough, flexible and efficient so that they are feasible in a variety of tunnel digging operations. However, the TBMs' effectiveness at breaking hard rocks is limited by issues such as the wear of the disc cutters in cutter head (Figure 1-2, **Hassani and Nekoovaght, 2011**). Replacement requires design to meet the different types of TBMs as well as transportation to the sites, which is very economically inefficient. Therefore improving the TBMs' performance by reducing disk cutters wear is key to reducing unnecessary costs while keeping the excavation process efficient.

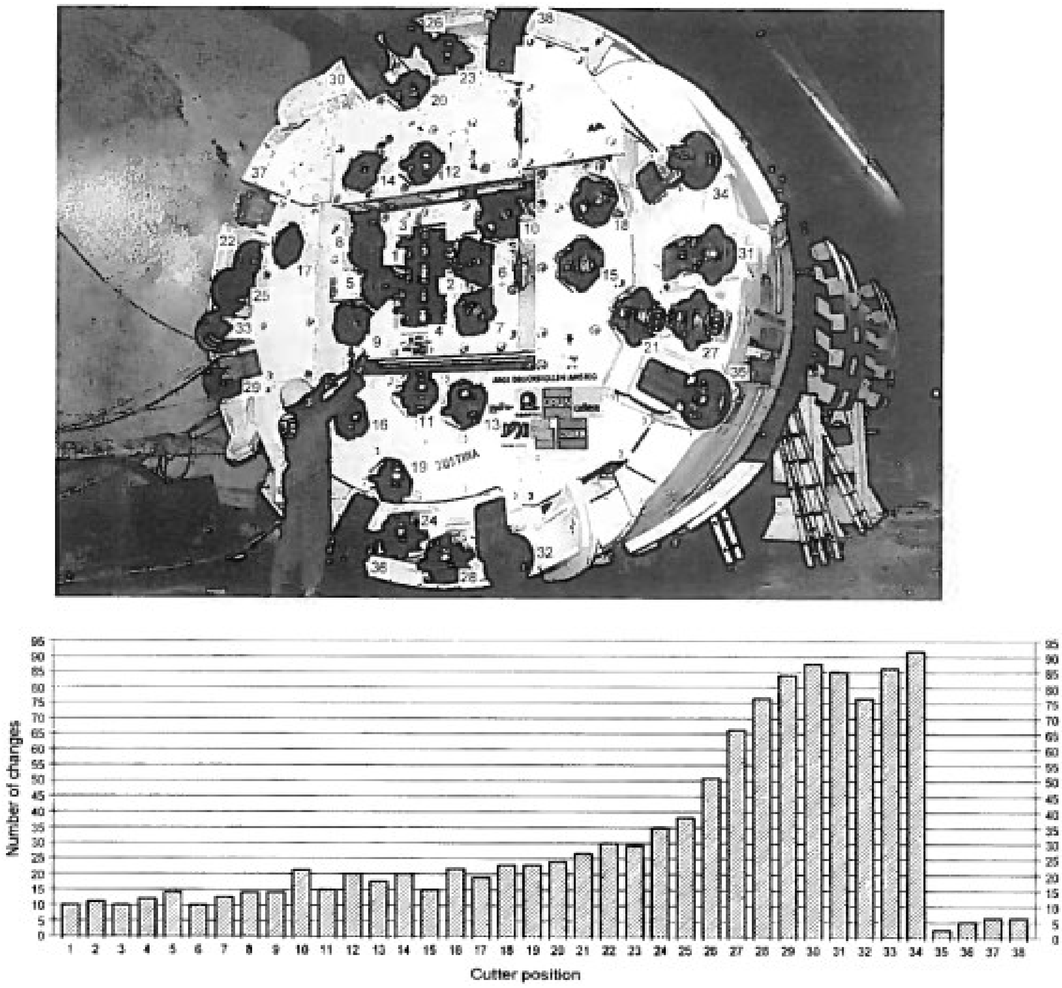

Figure 1-2. The degree of disc cutter wears in relationship to their positions on the cutter head (Maidl et al., 2008)

If the hard rocks can be "softened" prior to cutting, the cutting process would become much easier. Microwaves have been proved to be an effective treatment to make rocks more brittle (**Nekoovaght, 2009**), and therefore could be used as an ideal tool to preheat the rock wall ahead of the TBM. A schematic view about the prototype of the possible design of a TBM with microwave system is shown in Figure 1-3, left. Several radiating antennas are installed on the cutter head in combination with the disc cutters. The microwaves emitted from these antennas can penetrate the wall and heat it from inside. The front wall, side walls of the tunnel and cutter head of the TBM will form an enclosed space for microwaves to reflect to form standing waves that can heat the space. Once the areas have become fragile, the disk cutters will have significantly reduced wear (Figure 1-3, right)

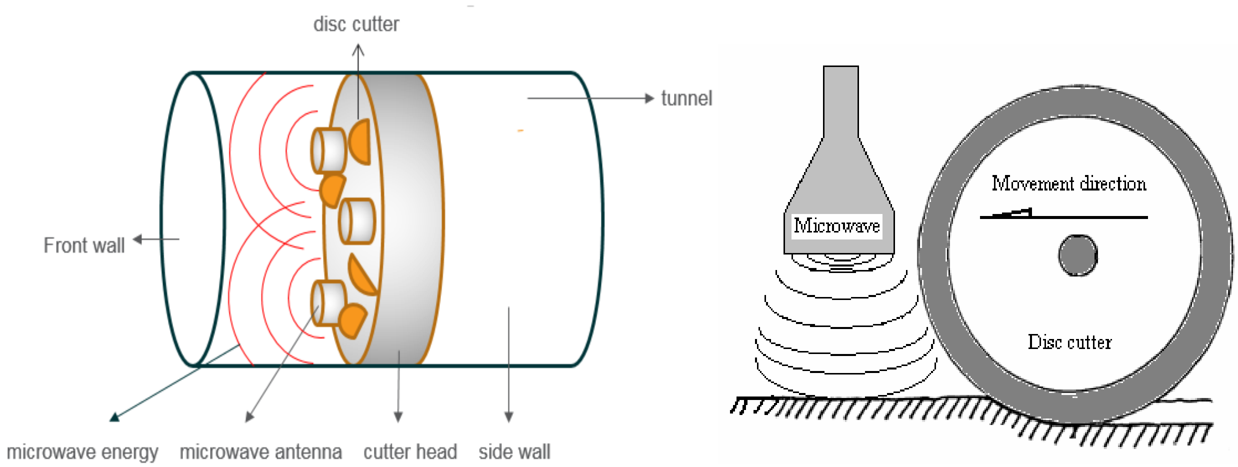

Figure 1-3. Antenna installation on the cutter head of a TBM (Hassani and **Nekoovaght, 2011)**

1.3. The goal of this thesis

Since a microwave-assisted TBM is merely a conceptual prototype, it requires a tremendous amount of research before it can be designed. Therefore it is unrealistic for this thesis to explain in details and with a high degree of complexity of such a system. As a small and basic component of a larger project on microwave-assisted TBMs that has been carried out in the mining department of McGill University, the main goal of this thesis is to analyze the temperature distribution inside basalt under the influence of microwave radiation in a laboratory environment.

Four major objectives are to be determined:

1. The influence of diameter to height ratio on temperature distribution in cylindrical basalt cores;

2. The influence of rock shape on temperature distribution using cubic and cylindrical basalt cores;
3. The influence of internal spacing on temperature distribution for cylindrical basalt cores;
4. If a relationship exists between microwave energy absorption and volume, and if a relationship exists between the temperature and volume, of cylindrical cores;

Chapter 2 in an introduction of theoretical aspects of microwave heating, followed by the design and methodology of the experiment in chapter 3, which is followed by the results and analysis in chapter 4, and the conclusions in chapter 5.

II. Theoretical Aspects of Microwave heating

2.1. Microwave definition, application and Maxwell Equations

A microwave is an electromagnetic wave with a wavelength between 0.1mm and 100cm and frequency between 300MHz and 300GHz (Figure 2-1). It is located between the FM broadcast radio and far infrared frequency bands in the spectrum. In free space, the speed of a microwave is the same as the speed of light, which is approximately 300000km/s.

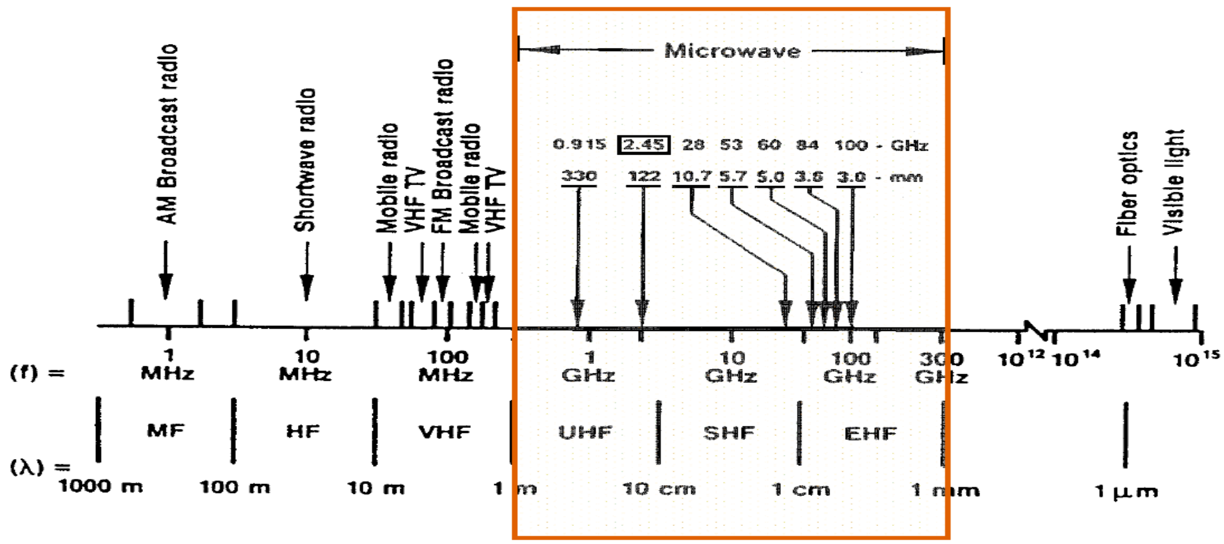

Figure 2-1. Microwave frequency band in electromagnetic spectrum (National Research Council U.S., 1994)

Applications of microwaves are usually divided into two categories, communications and heating. The advantages of using microwaves over other electromagnetic waves as a communication signal are (**Pozar, 2011**):

- high capacity transmission;
- high efficiency in radar applications
- multiple applications in areas such as remote sensing and weather forecast.

The advantages of using microwave for heating method are that (**Haque, 1999**):

- deep penetration yields good internal heating;
- selective heating is possible because different materials absorb microwave energy according to their dielectric properties;
- the high frequency can compensate for the deficiency of electromagnetic field intensity, saving electrical power; and
- microwave are highly efficient because heat is generated through energy transfer instead of heat transfer

Microwaves are composed by electric and magnetic fields that propagate in the form of wave (far field). The original four fundamental equations describing the relationship between the electric (E) and magnetic field (H) and electric sources are (**Maxwell, 1873**):

$$\nabla \times E = -\mu \frac{\partial H}{\partial t} \qquad 2.1(1)$$

$$\nabla \times H = \varepsilon \frac{\partial E}{\partial t} + J \qquad 2.1(2)$$

$$\nabla \cdot E = \frac{\rho}{\varepsilon} \qquad 2.1(3)$$

$$\nabla \cdot B = 0 \qquad 2.1(4)$$

Helmholtz developed the above equations into

$$\nabla^2 E + \omega^2 \mu \varepsilon E = 0 \qquad 2.1(5)$$

$$\nabla^2 H + \omega^2 \mu \varepsilon H = 0 \qquad 2.1(6)$$

E and H are the intensity of electric and magnetic field, μ is the permeability of the medium, ρ is the density of electrons, J is the current density, ε is the permittivity of medium and B is the magnetic flux. The solutions of equation 2.1(5) and 2.1(6) reveal that the electric and magnetic fields oscillate periodically with time and distance while propagating, can be found in many books (**Hayt and Buck Jr, 2011**; **Cheng, 2004)**. The appearance of a plane wave travelling in free space on z direction and having E field in x direction and H field in the y direction is shown in Figure 2-2.

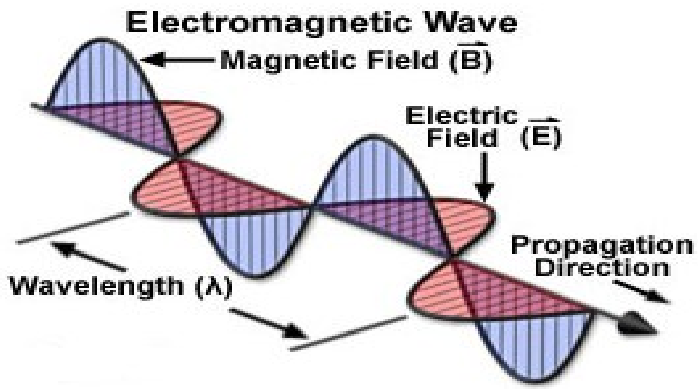

Figure 2-2. Plane electromagnetic wave propagating in free space (Davidson, 1998)

2.2. Dielectric properties and microwave heating mechanism

2.2.1. Dielectric properties

In terms of heating, dielectric properties determine how well a material is able to respond to the oscillation of electromagnetic field to generate heat. Every material has its own dielectric properties according to which they are generally divided into three classes: transparent, conductor and absorber (Figure 2-3). Transparent materials such as ceramics let microwaves penetrate completely without reflecting or absorbing any energy. Conductors such as aluminum foils completely reflect electromagnetic waves; they neither absorb energy nor let it pass through. Absorbers such as basalt reflect part of the energy and transmit the rest; the transmitted electromagnetic energy is eventually converted into heat and dissipates inside the material. For absorbers, dielectric properties depend on the frequency of the electromagnetic wave, and the composition, water content, temperature and density of the absorber material.

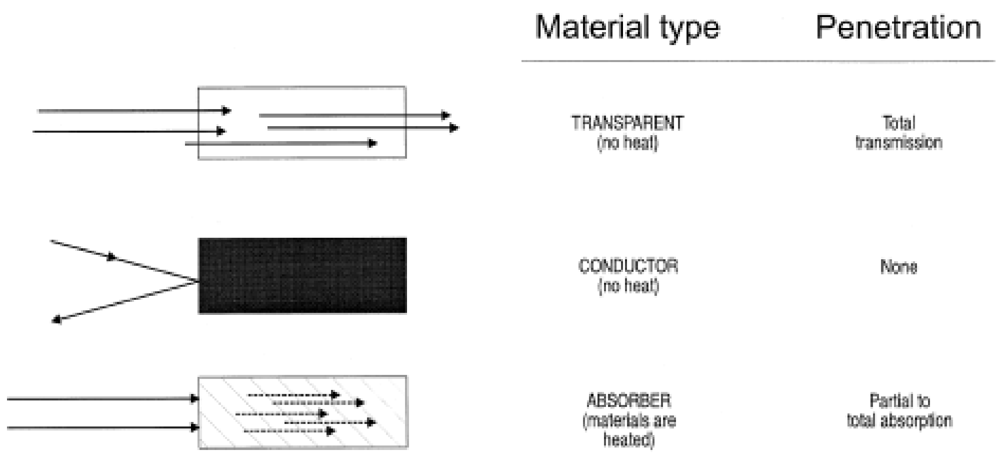

Figure 2-3. Three types of material based upon their response to incident electromagnetic waves (Haque, 1999)

The permittivity can be used to quantify the dielectric properties of a material, and possess the form:

$$\varepsilon^* = \varepsilon' - j\varepsilon'' = \varepsilon_0\varepsilon_r - j\varepsilon_0\varepsilon''_{eff} \qquad 2.2\ (1)$$

Where $\boldsymbol{\varepsilon}'$ is the dielectric constant, an indicator of the dielectric's ability to store electromagnetic energy as it is and $\varepsilon''$is the loss factor, an indicator of the dielectric's ability to convert electromagnetic energy into heat. ε_0 is the permittivity in free space, ε_r is the relative permittivity of the absorber, and ε''_{eff} is the loss factor of the absorber. The loss tangent

$$tan\delta = \frac{\boldsymbol{\varepsilon}''}{\boldsymbol{\varepsilon}'} \qquad 2.2\ (2)$$

is a measure of the effective loss of microwave energy over the energy stored by the materials. The bigger the loss tangent, the better the materials can absorb microwave energy.

2.2.2. Measurement of permittivity

Many techniques can be used to measure the permittivity between the frequency of 400 and

3000MHz, including: the *Roberts* and *von Hipple* (**1946**) method, X band techniques and perturbation methods (**Rzepecka et al, 1973**). At present, network analyzers are widely used to measure the dielectric constant and loss factor of a material. In example shown in Figure 2-4, the probe on the right is connected to a network analyzer through a coaxial cable. The probe emits electromagnetic waves generated by the network analyzer and receives reflected waves from the objects. The reflected waves are translated into electronic signals picked up by the computer, and the results can be read as digits.

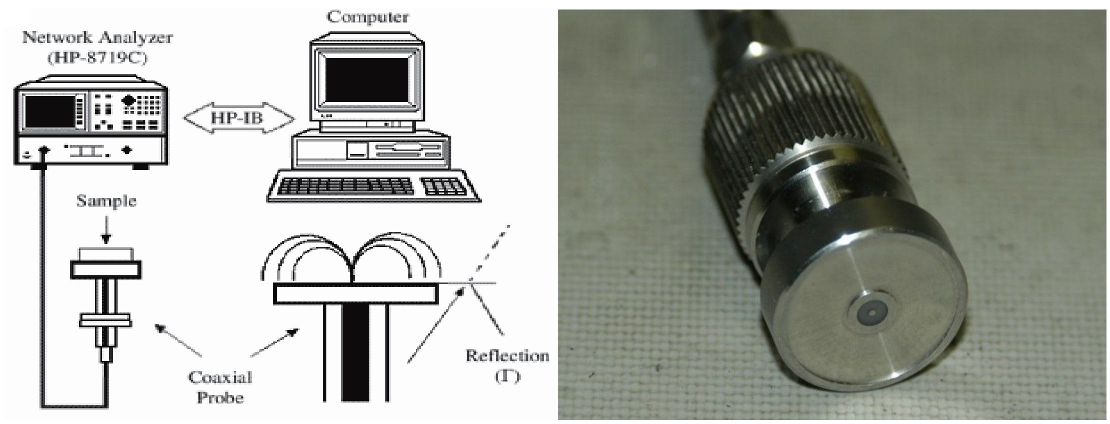

Figure 2-4. A set up using reflectometric technique to measure permittivity (de los Santos, 2003)

The basalt used in the present experiment was measured by using a network analyzer. It has the relative permittivity of $\varepsilon' = 8.6$ and $\varepsilon'' = 1.35$. Therefore the loss tangent is $tan\delta = \frac{\mathbf{1.35}}{\mathbf{8.6}}\ or\ 0.16$, which indicates that basalt is a very good electromagnetic wave absorber.

2.2.3. Microwave heating mechanism

Microwaves directly deliver energy into the materials via penetration to raise the internal temperature. According to **Metaxas and Meredith (1983),** dipoles tend to store energy when they have sufficient time to follow the electromagnetic field oscillation and release stored energy when they fail to follow faster oscillations. At a microwave frequency of 2.45GHz the dipoles eventually give up their pace to the oscillation of electromagnetic field; the energy stored is released and heat is generated. The transfer between electromagnetic energy and heat can be explained in the following equation (**Metaxas and Meredith et al., 1983**):

$$P = \frac{T - T_0}{t} \rho C V = \omega \varepsilon_0 \varepsilon_{eff}^{"} E_{rms}^2 V \qquad 2.2(3)$$

P is the power absorbed by the dielectric; T_0 and T are the initial and final temperatures of the dielectric before and after microwave treatment; t is the time of microwaving, ρ is the density of dielectric; V is the volume and C is the specific heat of the dielectric; ω is the angular frequency of microwave, $\varepsilon_0 \varepsilon_{eff}^{"}$ is the effective loss of dielectric; and E_{rms}^2 is the RMS value of electric field that penetrates into the dielectrics, which is constant in ideal situations.

Equation 2.2(3) has limitations because in reality the electric field is not constant in space within the material. It can only be used to analyze simple situations where the materials being heated are small in size and regular in shape (**Metaxas and Meredith et.al, 1983**).

2.3. Factors influencing dielectric properties of rocks

Abundant research on foodstuffs, daily products **(Bengtsson and Risman, 1971; Mudgett, 1979)** and non-daily products **(Basu, 2013; Amankwah and Ofori-Sarpong ,2011; Yoshikawa 1991, Wang and Schmugge, 2007)** has shown combination of electromagnetic wave frequency, and density, composition, temperature and most importantly, the moisture content of the material affects the permittivity.

Rocks tend to absorb less energy as the radiation frequency increases (**Ulaby, 1990**). Density accounted for about 50% of the real part dielectric constants variance but the author was not able to establish a relationship between density and loss factor. The dielectric properties of rocks are determined by the minerals that compose the rocks. Minerals that have different dielectric properties combine to form rocks with completely new dielectric properties (**Nekoovaght, 2009**). **Haque** (**1999**) found that most metal oxides, charcoals and sulphites are very susceptible to microwave energy absorption.

Water content in rocks is a very important factor influencing microwave absorption since the polarized water molecules rotate accordingly to the rapid change of the microwave frequency. Abundant empirical data and reports document that permittivity varies with moisture content of foodstuffs, and some light industrial and solid materials (**Tinga ,1969; Stuchly, 1972; Windle and Shaw, 1954**; **Hasted and Shah 1973**). Research regarding the relationship between dielectric properties and water content in rocks has generated ambiguous results because rocks are composed by minerals that have different hydrophilicity (**Olhoeft, 1976**). Rocks with good hydroscopicity are more likely to have their dielectric properties changed by water content than rocks with poor hydroscopicity **(Wuddivira, 2012)**. **Metaxas and Meredith (1983)** proposed a critical moisture content $\boldsymbol{M_c}$ below which the water absorption by materials is not sufficient to change the dielectric properties. For hygroscopic materials the critical moisture content is 10%-40% and for non-hygroscopic materials it is about 1%. A relationship between the water content and loss factor is shown in Figure 2-5.

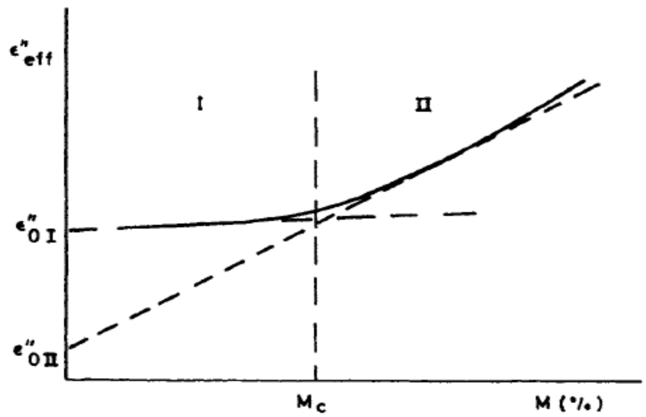

Figure 2-5. The effective loss factor as a function of moisture content (Metaxas, 1986)

The basalt used in experiment is considered as non-hygroscopic; therefore its water content does not a significantly influence its permittivity. Further, the microwave frequency is fixed at 2.45GHz and basalt is the only rock used in the present experiment, therefore the material density and composition doesn't vary among treatments.

2.4. Reflectivity of materials to microwave and the influence of internal spacing

2.4.1. Reflectivity and refractivity of materials to microwaves

Microwave reflection and refraction occur at the interface of two regions with different dielectric properties. When a microwave travels from one region to another a portion of the incident energy is reflected back by the interface and the rest is transmitted; both the reflected and transmitted waves carry less energy than the original incident wave. A typical scenario of incidence, reflection and transmission is shown in Figure 2-6 as the microwave strikes perpendicularly onto the interface of region 1 and region 2

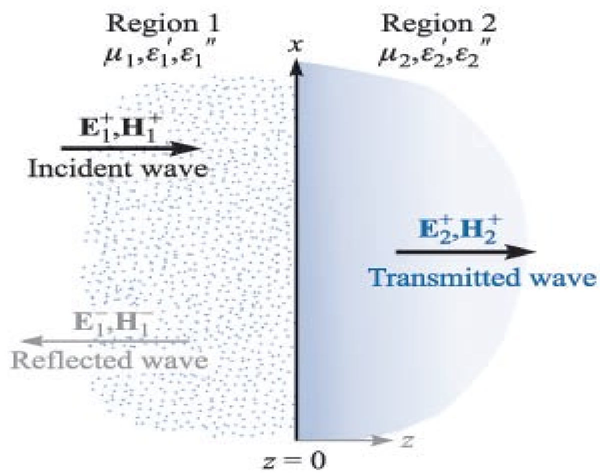

Figure 2-6. Incident, reflected and transmitted waves at the interface of two mediums when the incident angle is normal to the interface (Hayt and Buck Jr, 2011)

In Figure 2-6, the reflected wave overlaps with the incident wave to form a standing wave that has nodes and antinodes at fixed locations in region 1(Figure 2-7). The standing wave only oscillates with time, the peaks and troughs do not change with respect to distance. The standing wave has higher magnitude than both the incident and reflected waves.

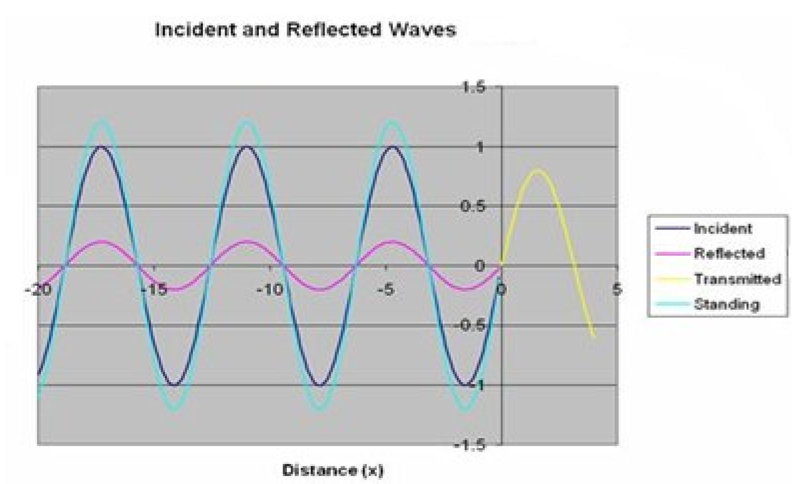

Figure 2-7. Standing wave formed by incident and reflected waves on the left side of the interface and transmitted wave on the right side of the interface (in yellow) (Mat lab animation)

On the other hand, when the incident wave doesn't strike the interface perpendicularly but rather at an angle, refraction occurs along with reflection (Figure 2-8).

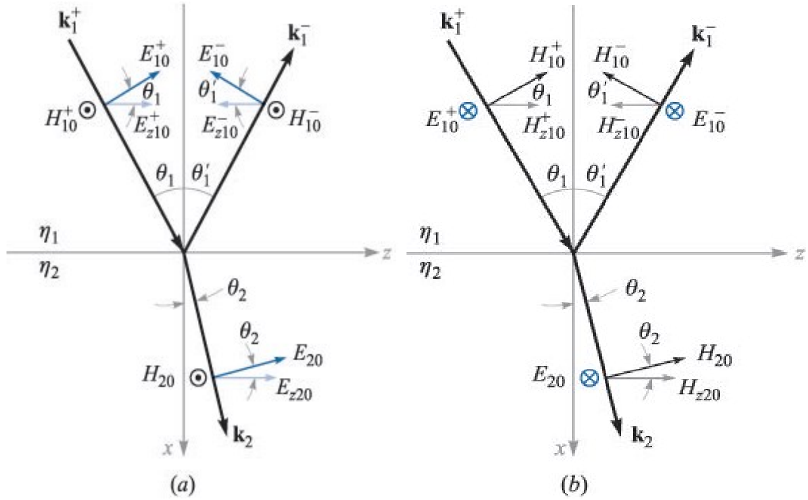

Figure 2-8. Microwave incidence on an oblique interface of 2 mediums: (a) TM mode, magnetic field doesn't have any component along the direction of wave propagation (b) TE mode, electric field doesn't have any component along the direction of propagation (Hayt and Buck Jr., 2011)

TE stands for transverse electric and TM stands for transverse magnetic. For a TE polarized wave, none of the vector components that are decomposed from electric vector field is in the direction of wave propagation. Similarly, for TM mode, none of the components decomposed from magnetic vector field is in the direction of wave propagation. The refracted part forms an angle $\boldsymbol{\theta_2}$with the X axis instead of continuing travelling along the direction of incident wave and the reflected wave also forms an angle $\boldsymbol{\theta_1^-}$ which is the same as the angle between the incident wave and the X axis.

Reflected and incident waves travelling in oblique directions can also form standing waves (Figure 2-9). Wave number1 and 2 both have their own wavelength, λ_0', which is the distance between two adjacent solid (or broken lines). When they overlap with each other new waves are formed with wave length λ_g indicated by the crossing points to two sets of parallel solid (or broken lines). The new wavelength is longer than the original one. Similarly but not indicated in

Figure 2-9, in the vertical direction, the crossing points of two sets of parallel solid and broken lines also form a wavelength that differs from the original one and the horizontal one. If the two waves indicated above are about to travel inward to or outward from the paper (or screen), another wavelength can be obtained in the direction going in and out of the paper (or screen).

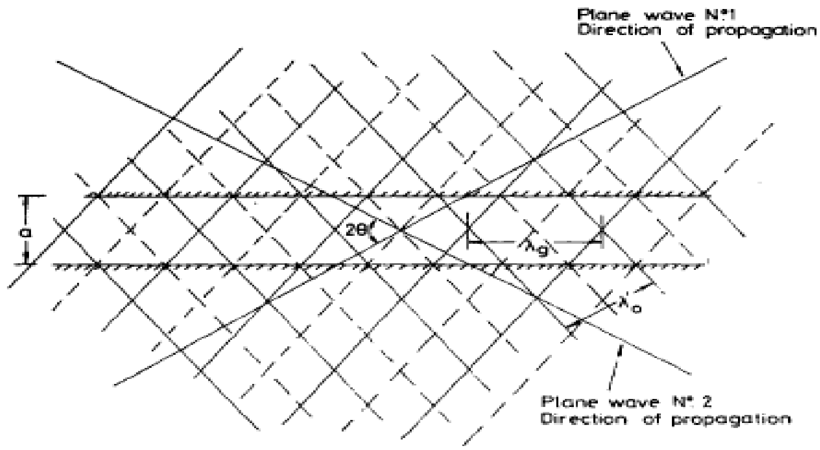

Figure 2-9. Overlap of two plane waves travelling in different directions (Metaxas and Meredith, 1983)

The reflection and refraction at the interface are essentially caused by the impedance mismatch between region 1 and region 2. The reflection coefficient is a parameter to determine the amount of electromagnetic fields reflected, which is

$$\Gamma = \frac{\eta_2 - \eta_1}{\eta_2 + \eta_1} \qquad 2.4(1)$$

η is the impedance of a dielectric and it is defined by the ratio of permeability and permittivity of the material, given by **(Hayt and Buck Jr, 2011)**:

$$\eta = \sqrt{\frac{\mu}{\varepsilon}} \qquad 2.4(2)$$

The relationship between the reflected and incident EM waves is therefore:

$$E_1^- = \Gamma E_1^+ \qquad 2.4(3)$$

And the relationship between the incident and transmitted EM wave is:

$$E_2^+ = (1+\Gamma)E_1^+ \qquad 2.4(4)$$

E_1^+ is the incident wave, E_1^- is the reflected wave, and E_2^+ is the transmitted wave. For incidence on the oblique interface, the reflection coefficient has become:

$$\Gamma = \frac{\eta_2 \boldsymbol{cos\theta_2} - \eta_1 \boldsymbol{cos\theta_1}}{\eta_2 \boldsymbol{cos\theta_2} + \eta_1 \boldsymbol{cos\theta_1}} = \frac{\frac{\eta_2}{\boldsymbol{cos\theta_1}} - \frac{\eta_1}{\boldsymbol{cos\theta_2}}}{\frac{\eta_2}{\boldsymbol{cos\theta_1}} + \frac{\eta_1}{\boldsymbol{cos\theta_2}}} \qquad 2.4(5)$$

for the TM mode and

$$\Gamma = \frac{\eta_2 \boldsymbol{cos\theta_1} - \eta_1 \boldsymbol{cos\theta_2}}{\eta_2 \boldsymbol{cos\theta_1} + \eta_1 \boldsymbol{cos\theta_2}} = \frac{\frac{\eta_2}{\boldsymbol{cos\theta_2}} - \frac{\eta_1}{\boldsymbol{cos\theta_1}}}{\frac{\eta_2}{\boldsymbol{cos\theta_2}} + \frac{\eta_1}{\boldsymbol{cos\theta_1}}} \qquad 2.4(6)$$

for the TE mode

$\boldsymbol{\theta_1}$ and $\boldsymbol{\theta_2}$ are the incident and refractive angles and are related by Snell's Law

$$\frac{\boldsymbol{\sin\theta_1}}{\boldsymbol{\sin\theta_2}} = \frac{\boldsymbol{n_2}}{\boldsymbol{n_1}} = \frac{\boldsymbol{k_2}}{\boldsymbol{k_1}} \qquad 2.4(7)$$

with

$$k = Im(j\omega\sqrt{\mu\varepsilon}) \qquad 2.4(8)$$

k is the propagation constant of microwave in the region and is determined by the dielectric properties of the material. *Im* indicates taking the imaginary part of the equation. The reflection coefficient between air and basalt samples in the present experiment is approximately 0.5(calculated in Appendix 2). This value indicates the microwave's electric field magnitude drops to half of its value when it travels from basalt to air or vice versa. The magnetic field, however, is not important because basalt doesn't have magnetic properties and the dipoles inside don't respond to the change of magnetic field.

2.4.2. Influence of spacing on microwave heating of materials

Discontinuities in a rock mass could be a boundary of different minerals, zones of closely-spaced and highly interconnected discrete structures, or cracks and porosities filled with air, other gases or liquids such as water (**Singhal and Gupta, 2010**). Common to all is that anisotropy is introduced into the rock mass. Thus, as presented in the above section, when microwaves encounter these discontinuities they are reflected and refracted by the interface of two different mediums.

The internal spacing between two cylindrical disks can affect microwave paths in a variety of way. When the spacing is very large, as indicated in Figure 2-10 (a), the microwave might die out before it reaches the bottom disk. When the wave is traveling from the side at an angle, total reflection can occur at the bottom surface of the disk on top; the waves are totally reflected back to the top disk as indicated in Figure 2-10(b). If this is true, the spacing has no effects because the microwave is not able to reach the disk at the bottom. When total reflection does not occur (Figure 2-10 c), some waves coming from the side can reach the bottom disk as shown by the blue arrows, but other waves can as shown by the red arrows. When the spacing is very large, waves coming from the top surface of the top disk are not able to reach the bottom disk due to refraction that occurs twice (Figure 2-10d). On the other hand, if the waves coming from the top penetrate into the top disk from areas away from the center, after they leave from the bottom surface of the top disk they are able to reach the bottom disk as shown in (Figure 2-10e).

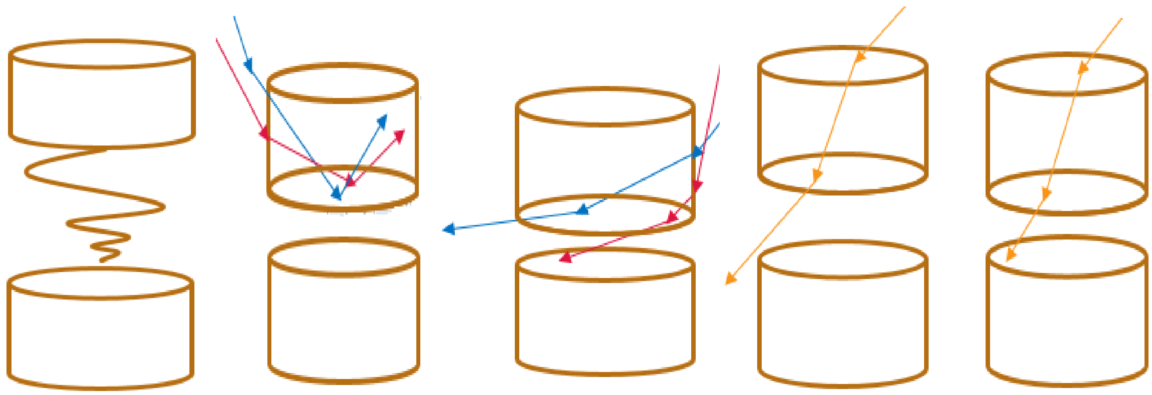

Figure 2-10. The influence of spacing affecting wave travelling path in a variety of ways

2.5. Power and penetration depth

Microwaves that travel in a lossy medium (absorber) will lose energy to the material. Therefore the electromagnetic field decreases as they travel deeper into the material. The wave form will appear as shown in Figure 2-11:

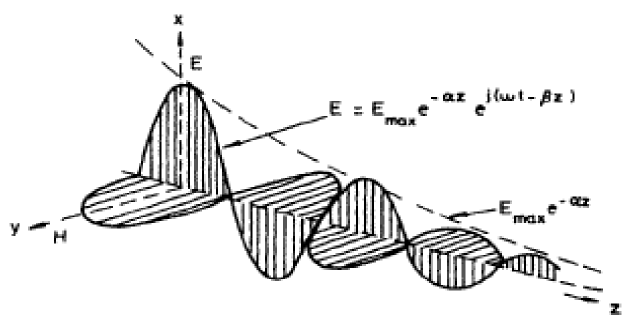

Figure 2-11. Propagation of plan wave in a lossy medium (Metaxas and Meredith, 1986)

The solution of Maxwell's equation for wave travelling in lossy medium for a plane wave travelling in z direction has become (**Hayt and Buck Jr, 2011**).

$$E = E_{max} e^{-\alpha z} e^{j(-\beta z + \omega t)} \qquad 2.5(1)$$

E is current magnitude of electric field, E_{max} is the peak value of the electric field, α is the coefficient of attenuation, and β is the propagation constant.

Equation 2.5(1) is a slightly modification of Maxell's equation's solutions with the introduced term of α, which determines the rate at which microwave energy can is dependent on the dielectric properties of the dielectrics:

$$\alpha = \omega\sqrt{\frac{\mu\varepsilon'}{2}}\sqrt{\sqrt{1+(\frac{\varepsilon''_{eff}}{\varepsilon'})^2}-1} \qquad 2.5(2)$$

And the propagation constant β also varies due to its dependence on the dielectric properties of the dielectrics:

$$\beta = \omega\sqrt{\frac{\mu\varepsilon'}{2}}\sqrt{\sqrt{1+(\frac{\varepsilon''_{eff}}{\varepsilon'})^2}+1} \qquad 2.5(3)$$

Since microwaves lose energy as they penetrate farther into the material, the energy they carry decreases in accordance to the distance from the surface of penetration. The penetration depth (D_p) describes the distance from the surface at which the power drops to 33% from its value at the surface:

$$D_p = \frac{1}{2\alpha} \qquad 2.5(4)$$

Microwaves heat materials by delivering electromagnetic power into the material. The electromagnetic power a material can absorb at the surface S is: (**Hayt and Buck Jr, 2011**)

$$P_{surface} = \frac{1}{2}\,Re\,(E \times H^*) \cdot S \qquad 2.5\ (5)$$

$P_{surface}$ is the power delivered by microwaves to the surface, S is the surface area, H^* is the conjugate of magnetic field and *Re* indicates taking the real part of the equation after calculation is done. The dot product indicates that only the tangential component of the electric and magnetic fields with respect to the surface are effective in transmitting energy into the material. The amount of microwave energy a type of materials can absorb therefore depends on a combination of the surface area and the angle at which the microwave penetrates from the surface.

Microwave power can be reflected at the interface of two different materials via impedance mismatch as described in the above section, and the transmitted power has a lower magnitude than the incident power. The transmitted and incident power at the interface is related by: (**Cheng, 2004**):

$$P_{trans} = P_{surface}(1 - |\Gamma|^2) \qquad 2.5\ (6)$$

P_{trans} is the transmitted power. Microwaves keep losing energy as they travel deeper into the materials. Depending on the distance the microwaves travel into the material, the relation between the powers they carry with respect to the powers on the surface is

$$P_{final} = P_{surface}(1 - |\Gamma|^2)\ e^{-2\alpha z} \qquad 2.5\ (7)$$

P_{final} is the power remaining in the microwaves as they are travelling inside the material and z is the distance from the surface. The penetration depth effects cause the outer areas of the material to be warmer than the inner areas because it is closer to the surface where microwaves penetrate. For the same materials, the larger the overall size, the less the energy can reach the center, leaving the center cooler than peripheral areas.

2.6. Microwave Heating System

A microwave heating system is able to generate, transport and deliver microwave energy to the load to be heated in the microwave cavity (oven) in a controllable way. One such system generally consists of the microwave generating component which includes one or multiple magnetrons, a protection component such as an isolator, a transporting component such as a waveguide, an impedance matching component such as a 3-stub tuner (optional) and the heating component such as a resonant cavity (Figure 2-12).

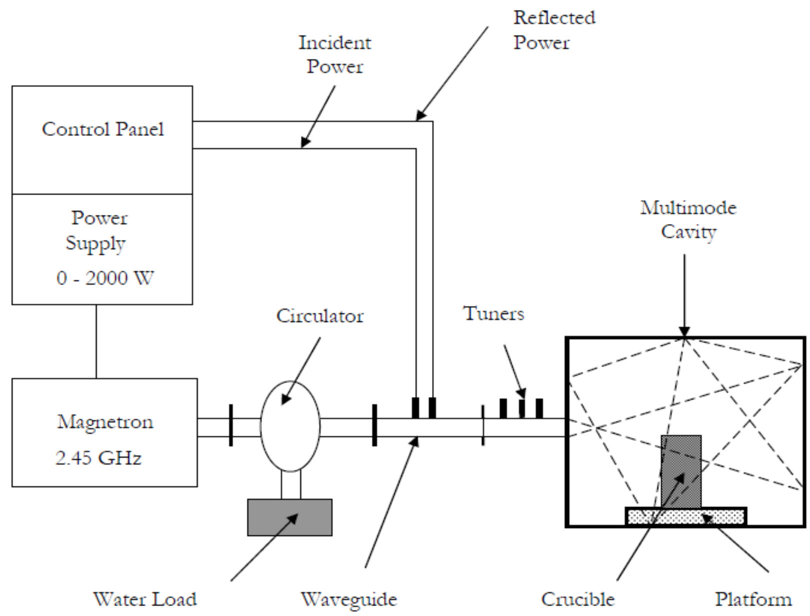

Figure 2-12. A microwave heating system (Pickles, 2009)

The magnetron is the most important part of a microwave heating system since it is responsible for generating the microwave. The electrons that are emitted radially from the cathode (Figure 2-13) during operation will experience both electric and magnetic forces exerted by the permanent magnets located on the top and at the bottom and circular cavities surrounded (Figure 2-13). These two forces drive the electrons to travel in a paracurve pattern by either boosting or reducing their speed. The accelerated electrons absorb energy from these tiny circular cavities and decelerated electrons give away energy**.** As a result, the increase in number of decelerated electrons and decrease of the accelerated electrons will form an electronic cloud shaped like a “spoke” in the space between the cathode and anode (Figure 2-13).The “spoke” shaped electronic cloud will constantly provide energy to the resonators to sustain its operation. The constant magnitude and polarity changing electromagnetic field at a certain frequency is picked up by the loops located on the wall of the resonator, coupled into an antenna and radiated into the waveguide as an electromagnetic wave.

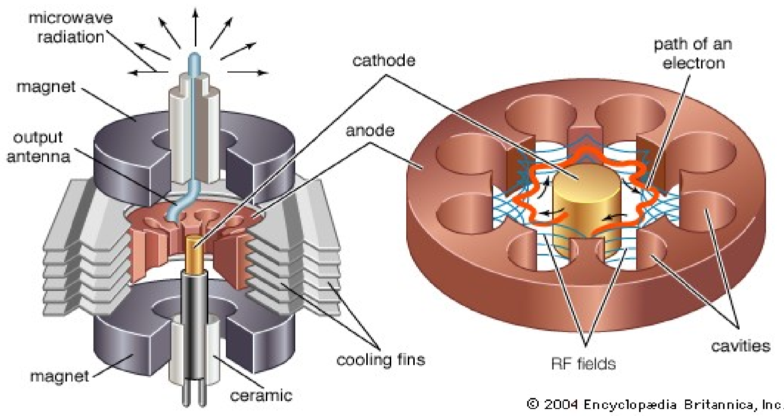

Figure 2-13. Magnetron and its internal structures (Copyright © 2007-2014, Mainland High School ISTF, Volusia County Schools)

The circulator is a three-port device that protects the source from being damaged by reflected microwave power resulting from the impedance mismatch between the magnetron and waveguide. A two port device with water load as dummy is sketched in Figure 2-14. The reflected power is absorbed by the water load to prevent the magnetron from overheating. However, the forward electromagnetic energy won't be affected by the load.

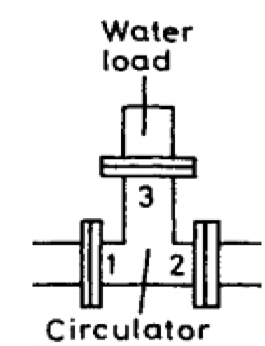

Figure 2-14. Schematic view of a two-port circulator with a water load (Lester, 1953)

A tuner can be adjusted to maximize impedance matching between the waveguide and resonator cavity and yield the most efficient power transmission. (Figure 2-15).The tubs on the tuner can be pushed in to different lengths to vary the structure of the tuner. The structure of the tuner is used to determine the efficiency of impedance matching. By making impedance of the tuner approach that of the cavity containing the load, the amount of reflected power by the load to achieve maximum power transmission is minimized.

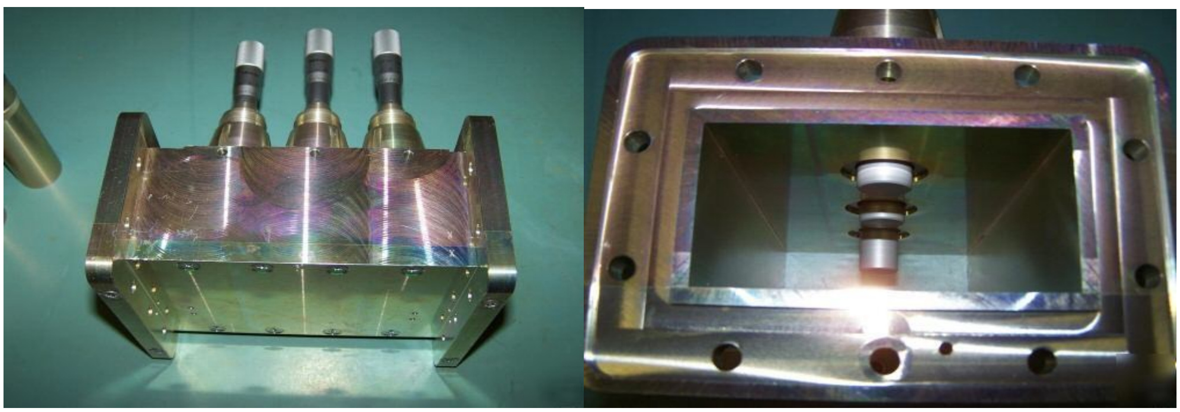

Figure 2-15. WR-340 Microwave stub tuner at 2.45 GHz, manufactured by Muegge, model number MW2101A-260EC

The waveguide collects the microwave radiated from antenna and delivers the energy in the desired direction. The most commonly used waveguides are rectangular and cylindrical (Figure 2-16). The walls of a waveguide are made of highly conductive materials such as aluminum, so that the electromagnetic waves can bounce off the walls to form standing waves in the cross section while propagating along the longitudinal section.

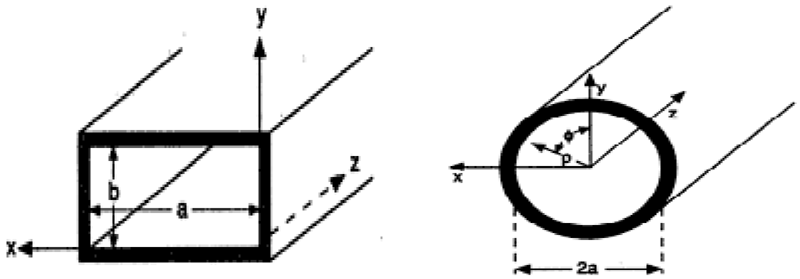

(a) (b)

Figure 2-16. A rectangular waveguide (a) with section plan view and a cylindrical waveguide (b) with section view (**Dorf, 2003**)

Electromagnetic waves propagate inside the waveguide in a pattern determined by the structure of the waveguide and source of excitation. For rectangular waveguides, two of the patterns at the cross and longitudinal sections corresponding to TM and TE modes are shown in Figure 2-17.

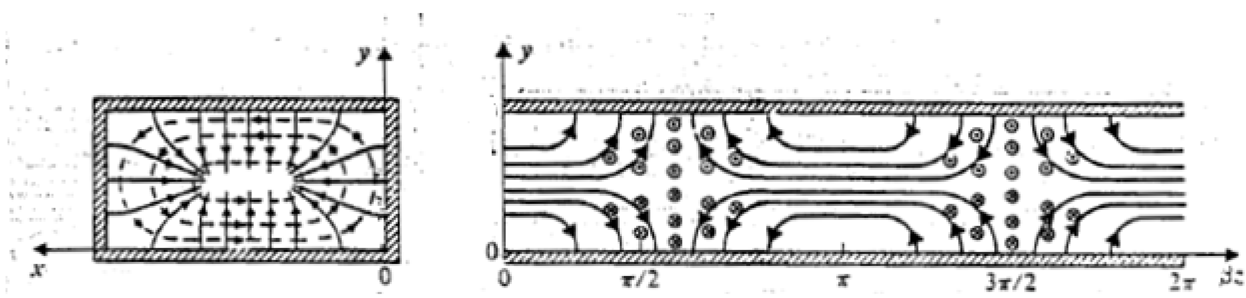

(a)

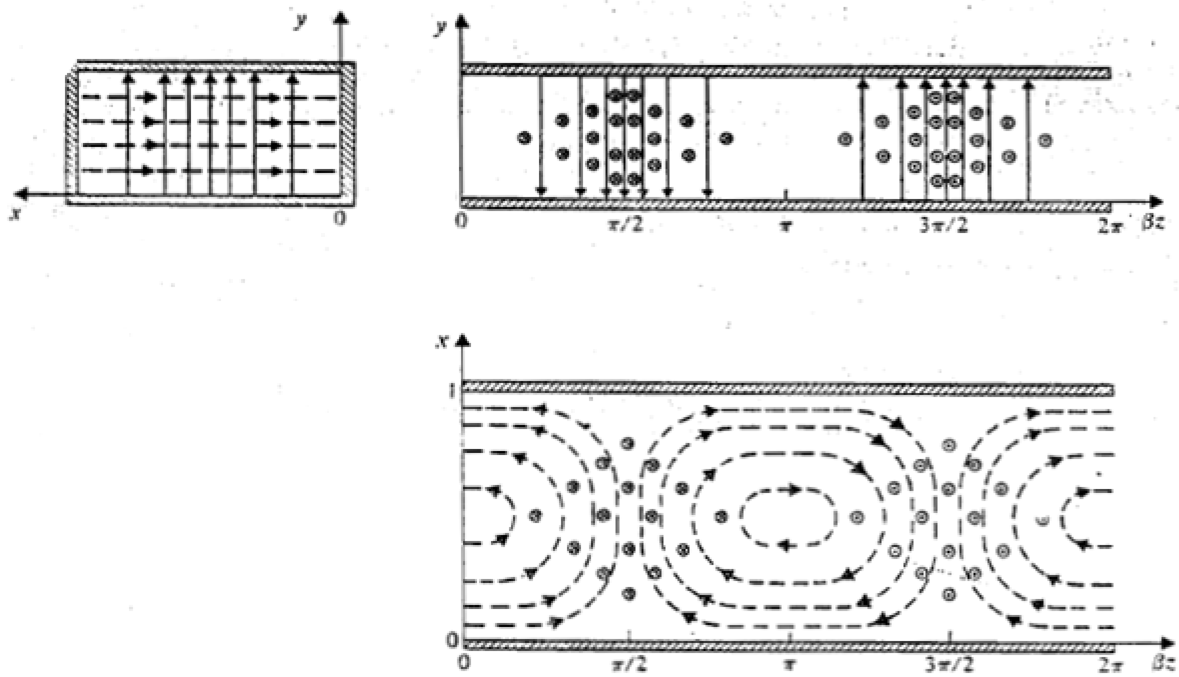

(b)

Figure 2-17. Wave patterns corresponding to TM_{11} mode (a), and TE_{10} mode (b) at cross and longitudinal sections of a rectangular waveguide. The solid line represents the electric field and the broken line represents the magnetic field (Cheng, 2004)

Similarly, for a circular waveguide, two of the patterns at the cross and longitudinal sections correspond to TM and TE modes (Figure 2-18). The electric and magnetic fields in an electromagnetic wave travelling in the waveguide are no longer transverse to the direction of propagation. Instead either TE or TM waves can exist in a waveguide, indicating at least one component of either the electric or magnetic field is in the direction of propagation. The numbers in the subscript in Figure 2-18 represent the mode of the wave, and are integral multiples of the half wavelength in each dimension, which are determined by excitation of the source and the dimension of the waveguide. A minimum frequency is required for the electromagnetic wave to successfully propagate from the entrance to the exit of the waveguide and this frequency is called the cut-off frequency. The cut-off frequency is also determined by the dimensions of the waveguides. The waveguide serves as a secondary antenna when radiating electromagnetic waves into the cavity. The boundary conditions at the interface of waveguide and cavity is defined by *Huygen's theorem* and *Love's Principle* (**Stutzman and Thiele, 1998**).

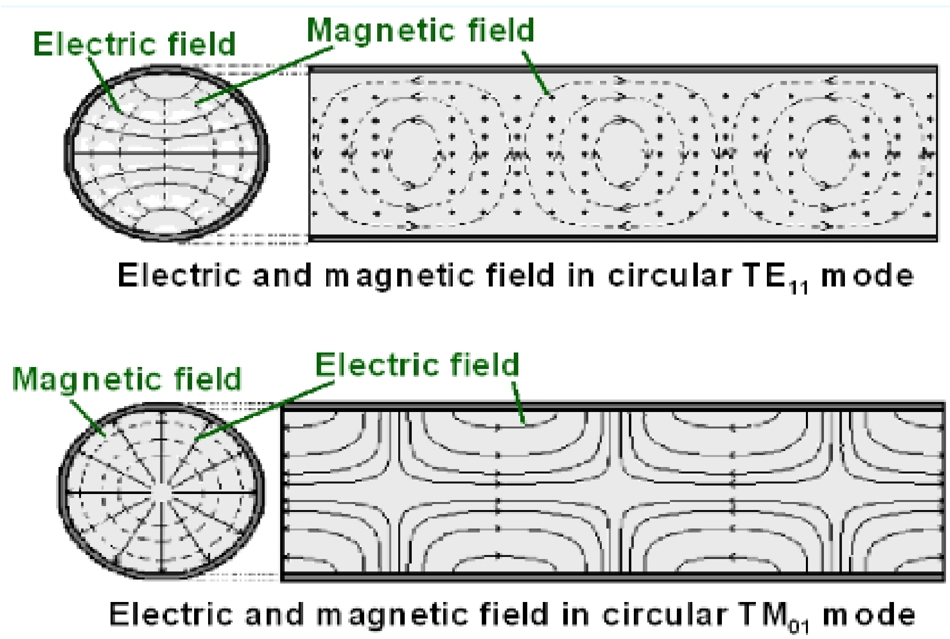

Figure 2-18. Cross and longitudinal section view of electromagnetic wave pattern for TE_{11} and TM_{01} mode in cylindrical waveguide (Hashizume & Ebara & Yusa Lab, 2014)

A load is placed in a cavity to receive microwave radiation. A cavity is a metal box enclosed by conductive walls in all dimensions (Figure 2-19). The waveguide delivers microwave energy through an aperture located on one of the walls (usually in the ceiling) and then the microwaves bounce off the walls to form standing waves that heat the load.

Figure 2-19. A multimode cavity with conducting walls and horn antenna connecting to a waveguide

Single-mode and multimode microwave cavities, the two types of cavities used in microwave heating differs in size. A single mode cavity is smaller only allows one specific mode to exist, multiple modes co-exist in a multimode cavity to form multiple modes of standing waves. The size of a single mode cavity is usually half of the microwave wavelength in at least two dimenstions, whereas a multimode cavity is usually several wavelenghs long in at least two dimensions. A mode inside a cavity represents the field or energy distribution inside. In a single mode cavity, the field distribution is very well defined according to Maxwell's equation and its solutions and pattern can be calculated analytically. A load to be heated can be placed at the areas where the field intensity is at a maximum, therefore it is very efficient for heating a low loss load . A waveguide with both ends closed by metall walls can be considered as a single mode cavity. On the other hand, the field distribution in a multimode cavity is chaotic. In the case of a rectangular box with dimensions *a, b* and *d* each mode must satisfy the equation (**Harvey, 1963**).

$$(\frac{m\pi}{a})^2 + (\frac{n\pi}{b})^2 + (\frac{l\pi}{d})^2 = (\frac{\omega}{c})^2 \qquad 2.6\ (1)$$

Where m, n, and l are the mode numbers (integral multiples of half wave length). Each combination of mode numbers represents a mode inside the cavity. The total number of modes is 50-60 in a cubic cavity operating at exactly 2.45GHz (**James, 1968**). The wave pattern in a multimode cavity is shown in Figure 2-10.

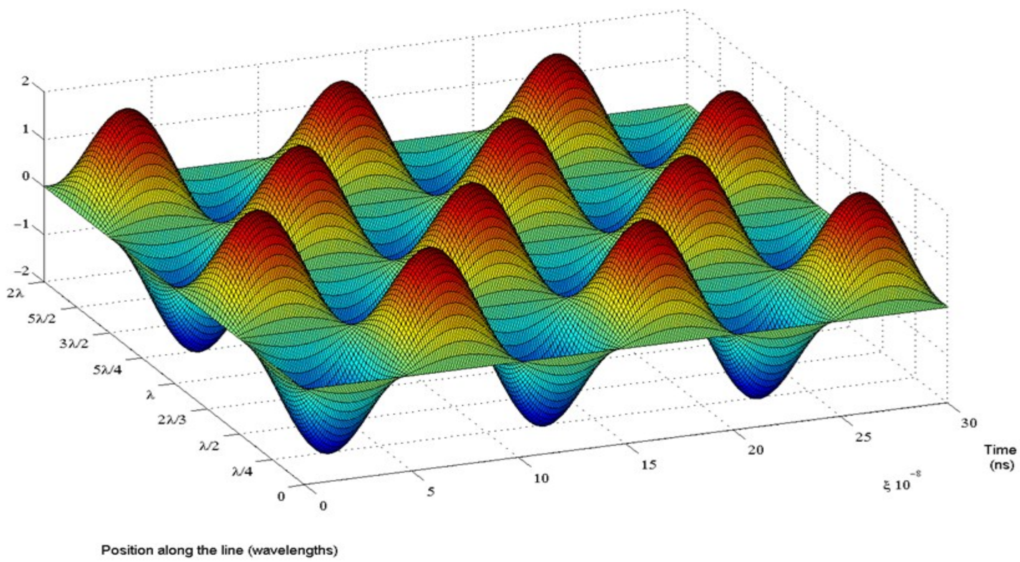

Figure 2-20. Standing waves formed by waves travelling at different directions inside a multimode cavity (DocFrankie.com)

Therefore multimode cavities are efficient in processing products in bulk and are mostly used in industrial applications. Some modifications can be made to improve heating uniformity for a multimode cavity, such as installation of a mode stirrer, placement of turn table or conveyor installation.

Another main difference between single and multimode cavity is the requirement for impedance matching between the waveguide and cavity. For a multimode cavity, a good impedance match is achieved as long as the standing wave ratio (VSWR), which is defined as:

$$S = \frac{1+|\Gamma|}{1-|\Gamma|} \qquad 2.6(2)$$

is lower than 3:1(**Metaxas and Meredith, 1983**) in the operating bandwidth of the generator. Materials chosen to be heated in a multimode cavity usually have a high loss factor, they tend to reflect little energy. On the other hand, impedance matching for a single mode resonator is more demanding since there is only one mode that can exist in the cavity. The mismatch between the waveguide and cavity will result in insufficient heating by reflecting a large portion of energy back to the waveguide.

III. Sample preparation and methodology

3.1. Sample preparation and equipment used in experiment

Basalt was chosen as the rock in these experiments because it is in expensive and ubiquitous, and more importantly, because it has a strong ability to absorb microwave energy. Sample preparation involved four steps: drilling, marking, cutting and grinding. Cylindrical cores were drilled out of a bulky cubic piece of basalt (Figure 3-1a) using a drilling machine (Figure 3-1b) and drill bits of 5.1, 7.1 and 10.1cm diameter. Cores were marked in such a way that each subsection was 1cm thick (Figure 3-1 c-d). Then each of the marked cores was cut into 1cm thick disk by a using chainsaw (Figure 3-1 e). Finally each disk was ground on both surfaces using grinding machine (Figure 3-1 f) to ensure the surfaces were smooth enough to minimize space between each disk when stacked.

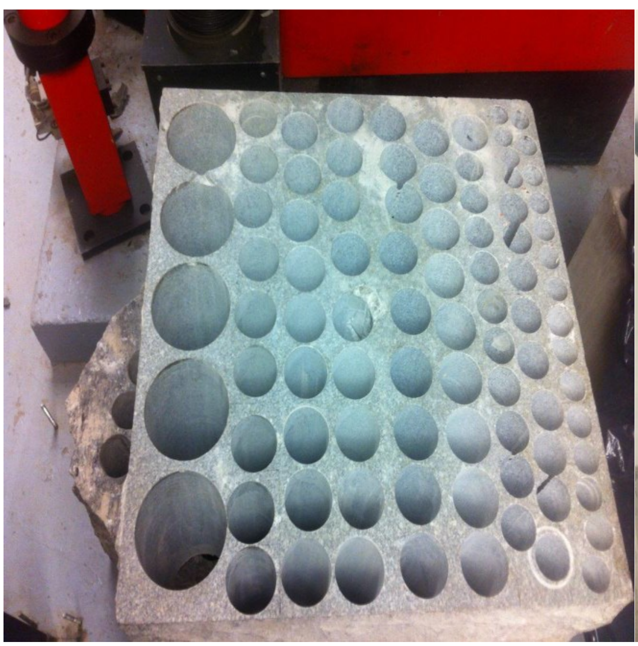

(a)

(b)

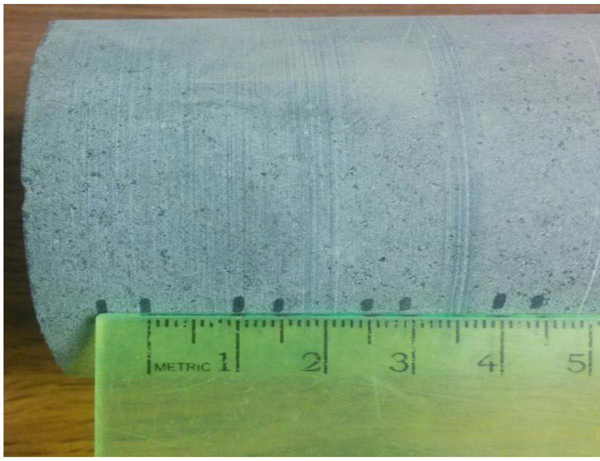

(c)

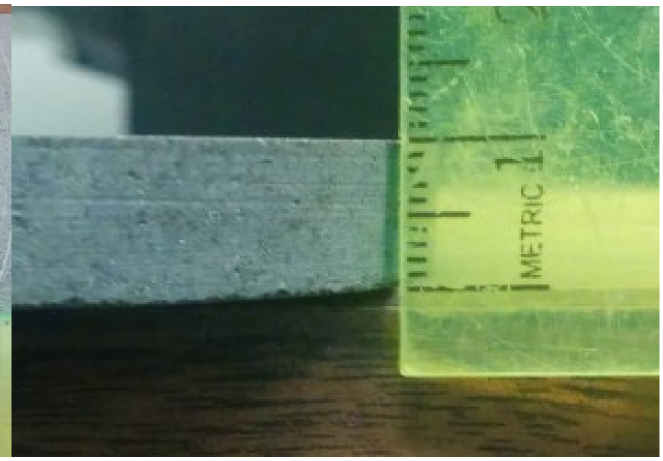

(d)

(e)

(f)

Figure 3-1. (a) Bulky cube from which cylindrical cores were drilled; (b) drilling machine used to drill the cores out of the bulky cube; (c) marked core in which the distance between each two dots is 1cm thick; (d) thickness of the each disk after cutting (e) chainsaw to cut cylindrical core into disks; (f) grinding machine to polish disk surfaces. (All the pictures shown in this section were taken in the GeoMechanics Laboratory of the mining and materials department of McGill University, which represent the real equipment and samples used in our experiment)

Similarly, square samples were cut from large slabs with a thickness of 2cm (Figure 3-2a-b). Further cutting risked breaking the samples. The square pieces were cut such that their side lengths are 4.5, 6 and 9cm and their surface areas are similar to cylindrical samples (Figure 3-2c)

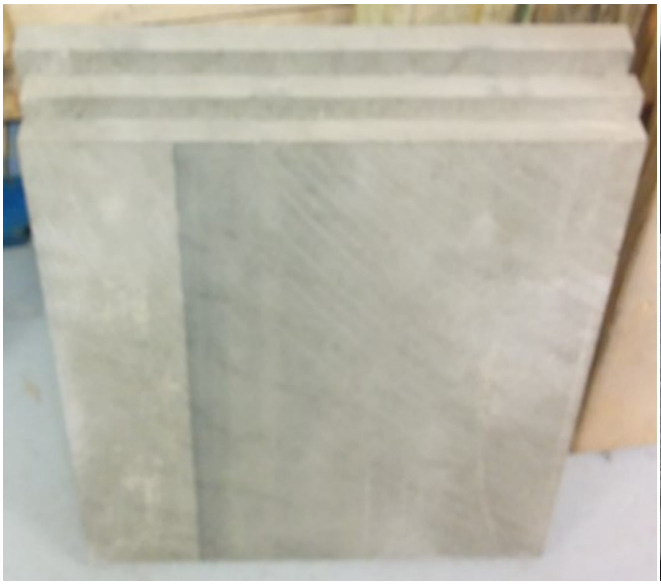

(a)

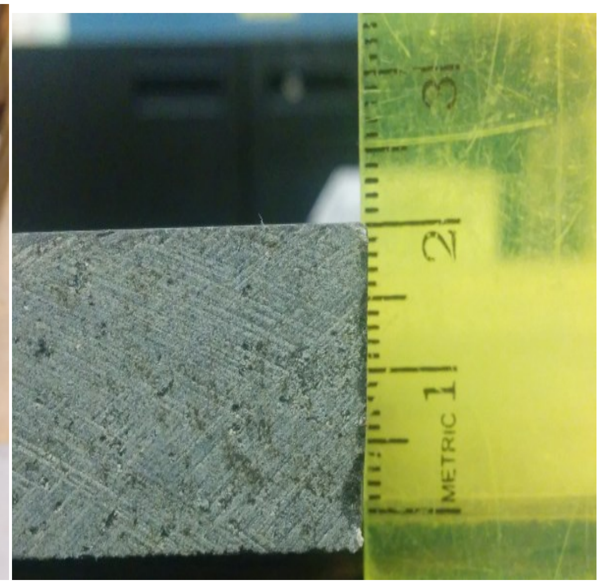

(b)

(c)

Figure 3-2. (a) Large basalt slabs from which smaller cubes were cut; (b) the thickness of each cubic disk; (c) square pieces and cylindrical disks have similar surface area

An infrared thermometer with laser aided aiming was used to measure the temperature of each disk (Figure 3-3, left). By knowing the amount of radiation and the emissivity of the samples, which is 0.97 for basalt, the temperature of the sample can be determined. The thermometer converts the radiated power of the sample into an electric signal displayed in the units of temperature on the screen. The accuracy is determined by the distance-to-spot ratio.-For instance, if the ratio is 10:1, measurement of the disk 25cm away will average the temperature over an area with diameter of 2.5cm inch. Therefore the temperature of each disk in experiments is the average of all the 17 spots as shown in Figure 3-3 right.

Figure 3-3. The infrared thermometer (left) area on basalt disk over which temperature is averaged (right)

A multimode cavity microwave oven with dimensions of 20 x 20 x 20cm was used to heat the basalt samples (Figure 3-4 left). The cavity has three conducting walls located on the left, right and in the back. The ceiling is plastic that is transparent to microwaves. The floor is made of ceramic that is also transparent to microwaves and serves to insulate the cavity. Two antennas on the top and one at the bottom radiate microwaves into the cavity. The two antennas on the top are perpendicular to each other to create a phase angle difference of 90° between the microwaves radiated from each antenna (Figure 3-4 right). During operation, all three antennas are rotating and radiating microwaves, creating a chaotic but relatively uniform wave distribution inside the cavity. Since there are two antennas on the top of the cavity, the energy concentration inside is stronger in the top half of the cavity and weaker in the bottom half of the cavity.

Figure 3-4. The microwave cavity and two antenna perpendicular to each other located on the ceiling of the cavity

3.2. Methodology

3.2.1. Evaluation of the difference between intact and stacked cores

To evaluate the temperature distribution of a core, the temperature of each disk was measured after microwave treatment. However, there was concern that a core created by stacking individual disks might not behave the same under microwave treatment as an intact core (Figure 3-5). The very thin layer of air between each disk serves as another medium, making the core a discontinuous object.

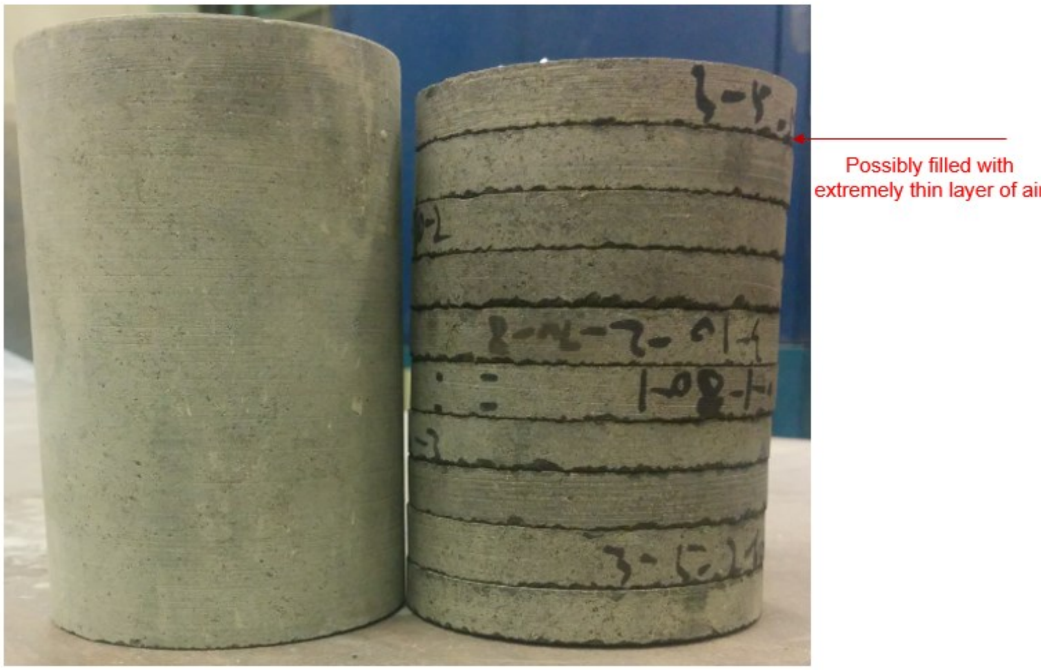

Figure 3-5. The difference between an intact core and core created by stacking individual disks

Theoretically, as long as the interface between basalt and air exists, it will influence the temperature distribution throughout the core because:

1. microwave coming from the side of the core can be totally reflected by the interface as shown in Appendix 3; and
2. the thin layer of air introduces impedance mismatch (see section 2.5) between itself and basalt, thus the amount of microwave energy that can reach the center of the stacked core is less than the amount when the core is intact.

The wave distribution in multimode cavity used is completely chaotic and conduction plays an additional role in changing the temperature distribution within the core. Therefore, the experiments were conducted with the assumption that the stacked core is the same as an intact core, as long as each disk in stack is completely contact with the disks below and above it, and the edges of the disk are perfectly aligned vertically. Under this premise, four experiments were conducted, as described in the following four sections.

3.2.2. Influence of diameter to height ratio on temperature distribution in cylindrical cores

To test the influence of size of a cylindrical core on the temperature distribution after microwave treatment, disks were divided into three groups according to their diameters (Table 3-1, Figure 3-6): 5.1, 7.1 and 10.1cm. For each diameter, disks were stacked into cores of 5, 8, 10, 13 and 16 cm(recall each disk is 1cm)

Table 3-1. Grouping of cylindrical cores according to diameter

		Diameter (cm)	
	5.1	7.1	10.1
	5	5	5
Height (cm)	8	8	8
	10	10	10
	13	13	13
	16	16	16

Figure 3-6. Cylindrical cores were grouped by three diameters (left), and for each diameter, disks were stacked to form 5, 8, 10, 13 and 16 cm cylinders (right)

Each core was microwaved for 90 sec, the temperature of each disk in each core was measured, and a trend line of temperature distribution for that core was plotted. Each core was microwaved twice with a cooling period in between treatments. The average temperature of two tests was reported. The standard deviation of the test means were also calculated in excel and represented by error bars on the temperature distribution trend line.

3.2.3. Shape influence on temperature distributions between cylindrical and cubic cores

To test the influence of shape on the temperature distribution in basalt after microwave treatment, cubes with widths of 4.5, 6, and 9cm and thicknesses of 2cm were tested. Only two heights were compared with cylindrical cores: 10cm and 16cm. The cubic disks were categorized according to their side length and height (Table 3-2, Figure 3-7). Treatment, temperature measurement and results reporting followed the same procedure as described above.

Table 3-2. Grouping of cubic cores according to side length

		Width(cm)	
	4.5	6	9
Height (cm)	10	10	10
	16	16	16

Figure 3-7. Cubic disks were grouped by side length (left) and for each side length the disks were stacked to form 10 and 16cm cores (right)

3.2.4. The internal spacing influence on microwave heating of cylindrical cores

To test the influence of air spaces on the temperature distribution in basalt after microwave treatment. Two separate tests were carried out. The first test used 7.1cm stacked cores to investigate whether 1mm spacing between each layer of the core affected temperature distribution relative to the cores of the same height with no spacing between layers (Figure 3-8). Spacing between layers was created by inserting very thin pieces of aluminum screening in each layer. The 10 cores were microwaved for 90,60,30,20 and 15 sec separately. The mean of two microwave treatments was reported as described above. Cores with spacing are regarded discontinuous, because some other mediums such as air are introduced into them. These discontinuities can reflect and refract microwave in the ways introduced in section 2.4. Whereas continuous cores as a whole won't have much internal reflections and refractions taking place inside. Besides reflection and refraction, the discontinuity can hinder the conduction process by creating insulation layer in between each disk. Therefore cores without spacing are able to conduct heat much better across disks than the core with spacing in each layer. The discontinuity also gives space for microwave to "squeeze" into the very tiny spacing to heat the surfaces of each layer. All these factors contribute for the different temperature distributions between cores with and without internal spacing.

Figure 3-8. Two 10-layer cores without (left) and with (right) 1mm air spacing between each layer

The second test investigated how the varying of spacing between layers in a core influences the temperature distribution in the core. Aluminum foil was wrapped around the 5-layer core such that only the top surface of the top disk was exposed to microwave radiation; the remaining disks were exposed to microwave that penetrated the top disk. The spacing between the top and second disks were then changed to observe the effects on heating the rest of the disks. The spacing tested were 0, 1, 4, 10 and 20mm (Figure 3-9 and Figure 3-10).

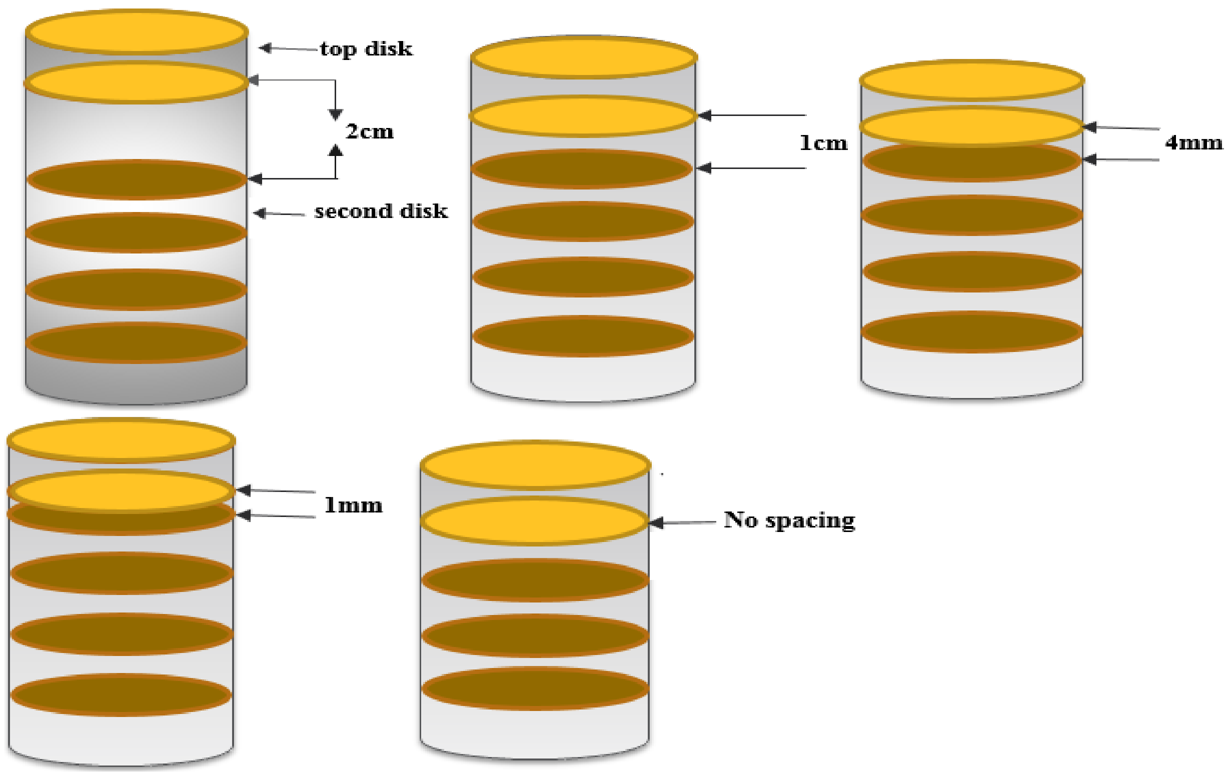

Figure 3-9. Spacings between the top and second disk in 5-layer core (graphs are generated using power point)

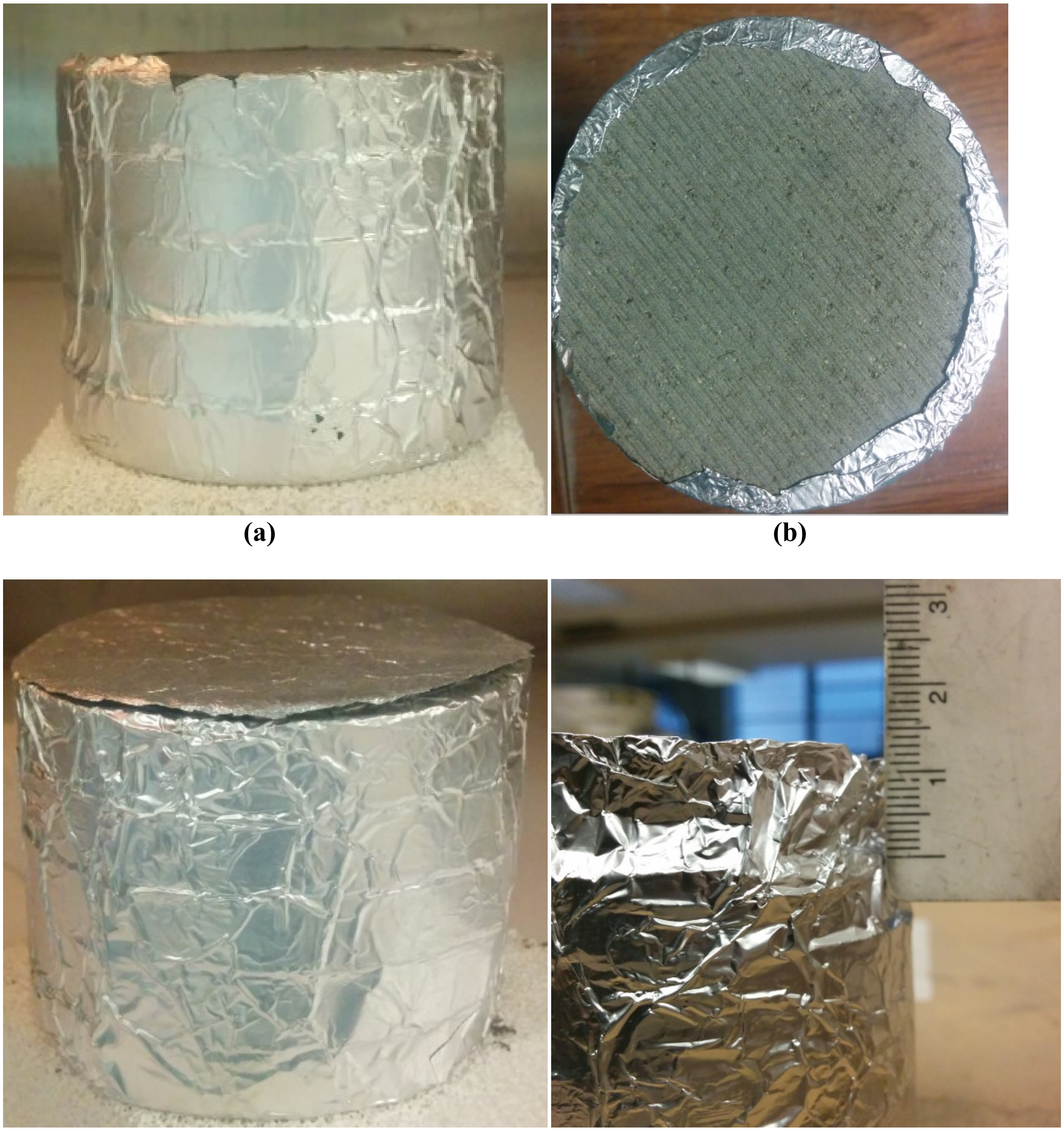

Figure 3-10. Laboratory setup to test the effects of varying spacing on heating of basalt core: (a) no spacing between top and second disk; (b) top disk is exposed to microwave radiation; (c) one side of the core covered by aluminum foil to block microwaves; (d) 1mm spacing between the top and second disk as an example

The 1mm spacing was created using the aluminum screening (Figure 3-11a). The other spacings were made with ceramics (Figure 3-11 b-c). Each core was microwaved twice for 30 and 60 sec. The mean of two measurements was reported, as described above.

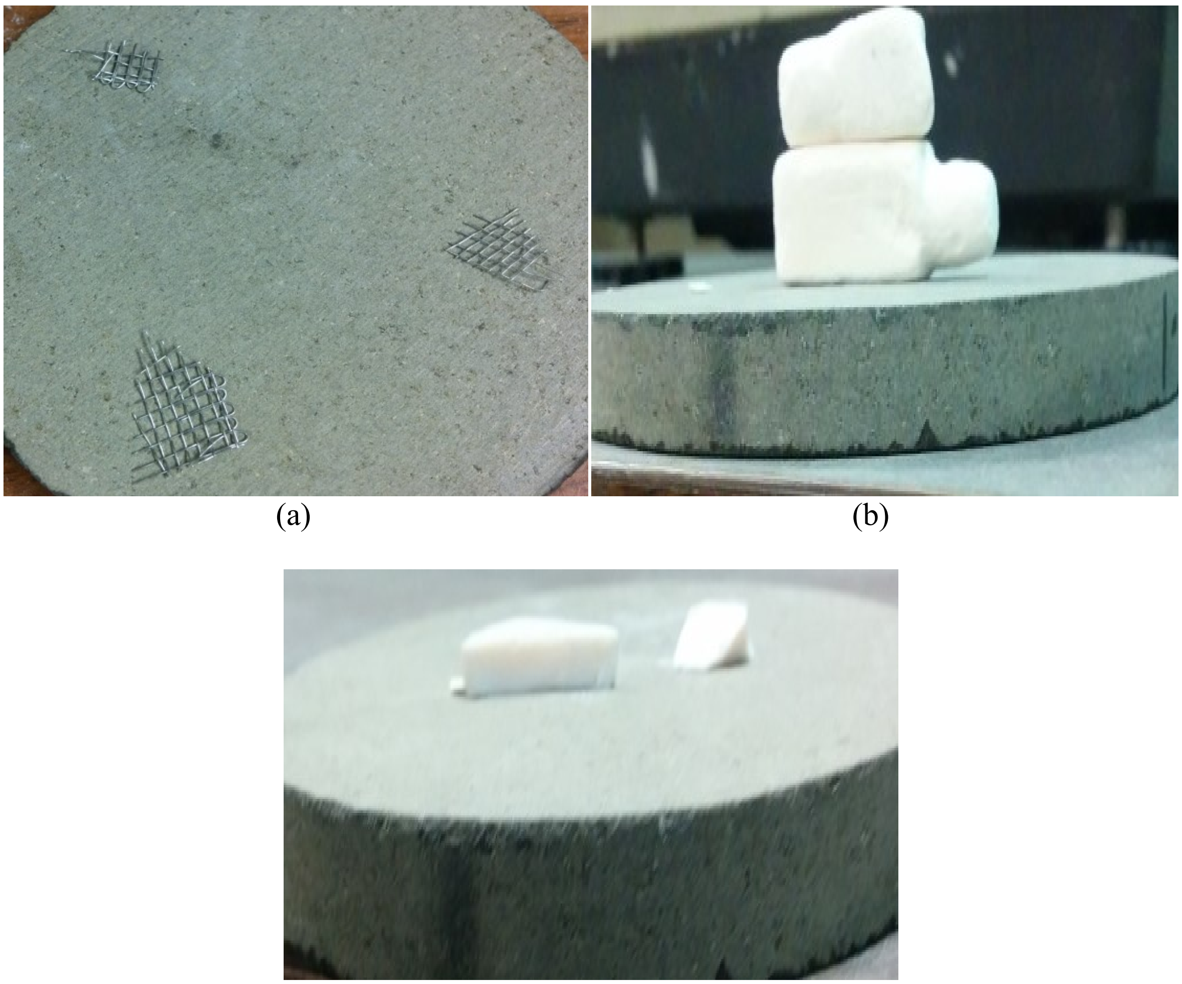

(a) (b) (c)

Figure 3-11. Varying spacings created with (a) 1mm pieces of aluminum screening; (b) 10mm thick ceramic bars and (c) 4mm ceramic snippet

3.2.5. Correlation between microwave energy absorption and temperature versus volume of cylindrical cores

The relationship was quantified between microwave energy absorption and temperature- and volume of the cores. The volumes of the 5.1cm, 7.1cm and 10.1cm diameter cores with 5cm, 8cm, 10cm, 13cm, and 16cm of height were calculated. For each disk, the energy absorbed is calculated according to the equation 2.2(3) (see equation 2.2(3)). Then the total energy absorbed by the core is therefore the sum of energy absorption by each disk in the core. The correlations were analyzed using regression method, which established the relationship between variables as basis for forecasting. If the correlation factor of a trend line is 1, it indicates a perfect match between the trend line and data; the future output can be predicted. If the correlation factor is smaller than 1, then the higher the correlation factor, the better the data can fit in trend line. For the correlation between power absorption and volume, the dependent variable or output is the power absorption and the independent variables or inputs are the final temperature and volumes of the cores. These three variables form a non-linear multiple regression system which can be used to estimate future output with available inputs and a trend line. For the correlation between temperature and volume, volume and power absorption are the independent variable. The temperature is the dependent variable. Excel has mathematical package to establish the most fit trend lines for the data available and this advantage was taken to analyze the experiment results.

IV. Experiment Results and Analysis

4.1. Temperature distribution for cylindrical cores

The Y axis represents temperature and the X axis represents the number of disk counting from bottom to top. For all disks in the core, the temperature was highest for the smallest diameter core, and lowest for the largest diameter core.

5cm cylindrical core had the highest temperature in the middle disk, regardless of the disk diameter (Figure 4-1). The electromagnetic energy in microwaves coming from the top and bottom was not significantly reduced after microwaves penetrated the top and bottom disks, therefore it was able to reach the disk in the middle with high intensity; meanwhile, microwaves coming from side overlapped with those coming from top and bottom to form a standing wave which resulted a peak temperature in the middle of the core.

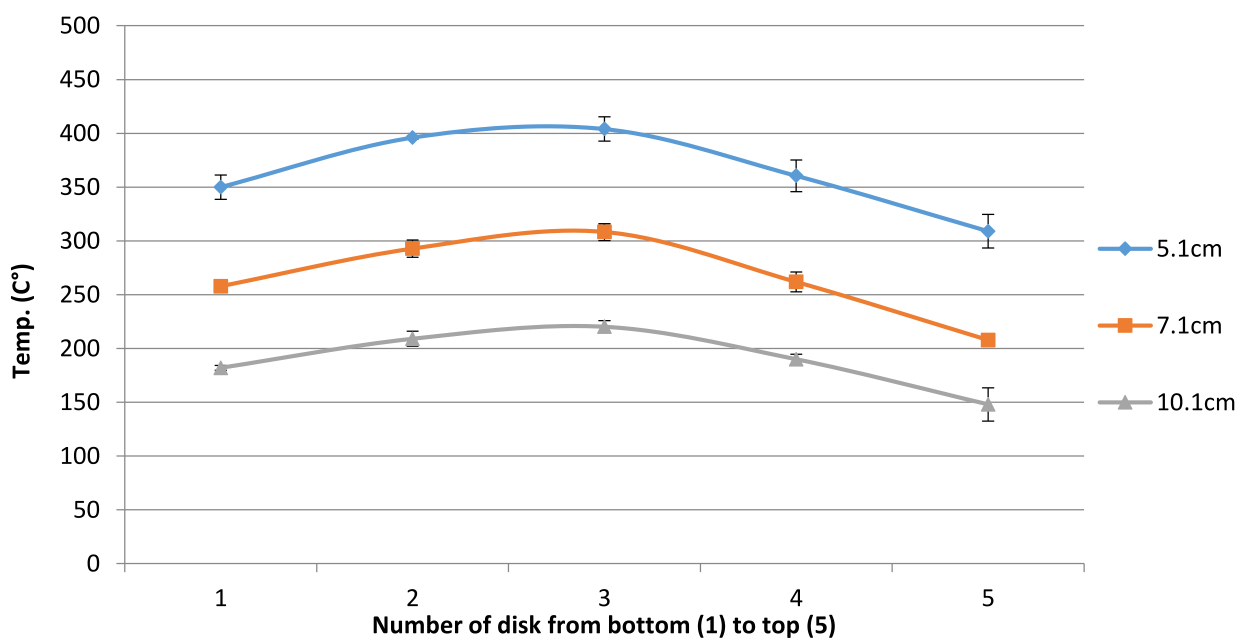

Figure 4-1. Temperature distributions of 5cm tall cores with three diameters after microwave treatment for 90 sec

Temperature peaks in cores with 8cm height shifted towards the top of the core when the diameter was 5.1 or 7.1cm, but remained in the middle of the core when the diameter was 10.1 cm, shown in Figure 4-2. At this height, microwave energy coming from the top and bottom of the cavity had less influence on the disks in the middle because penetration depth is limited. The relative influence of microwave coming from the sides, as well as conduction, was higher in 8cm than 5cm cores. The disks in the middle of the core were most likely heated by the wave coming from the sides as well as through conduction from adjacent disks. In disks 5 through 7, the temperature increased because radiations from the two rotating antennas installed in the ceiling of the cavity provided stronger electromagnetic field near the top half of the core than in the middle and bottom. Again, temperatures were higher in smaller diameter than larger diameter disks, regardless of position in the stack. For the largest diameter core, the temperature distribution is the smoothest, likely because the conduction rate is proportional to the surface area of the disk (Appendix 4). Larger surface are meant heat was conducted more rapidly to adjacent disks.

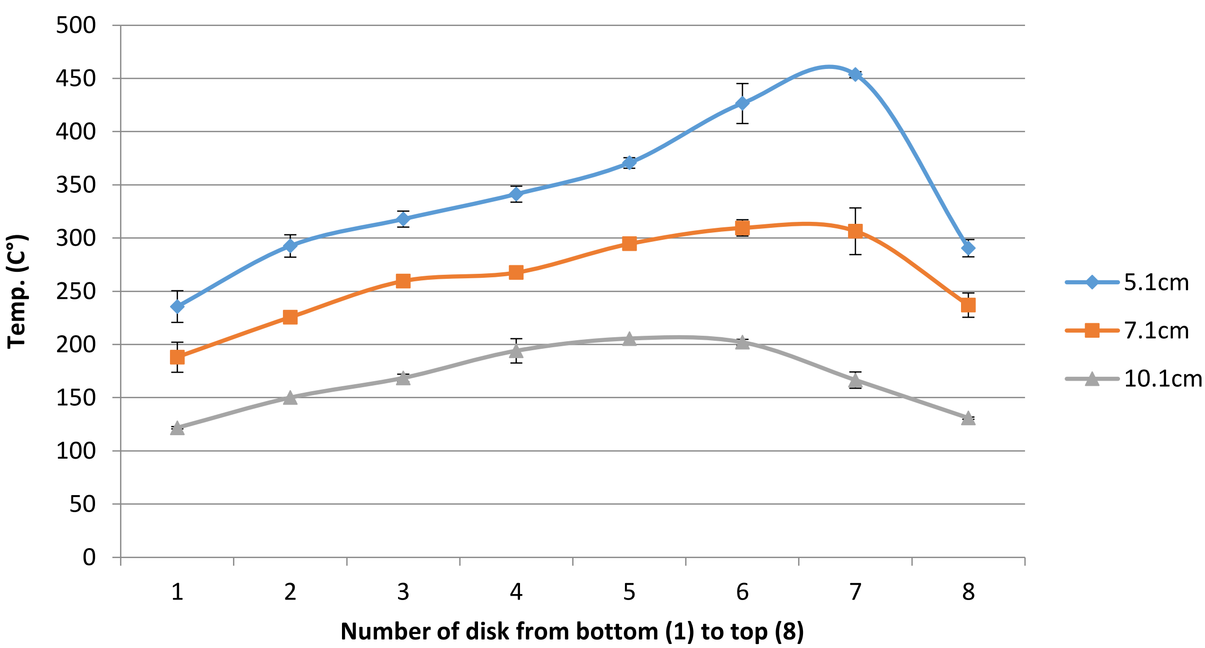

Figure 4-2. Temperature distributions of 8cm tall cores with three diameters

At 10cm, two peaks with different amplitudes were seen in the 5.1cm and 7.1cm diameter cores whereas only one peak was evident in the center of the 10.1cm diameter core, as shown in Figure 4-3. The stronger peak in the 5.1 and 7.1 cores was again due to higher microwave energy concentration in the top half of microwave oven. The temperatures through disk 3 to disk 5 decreased in Figure 4-3 instead of increasing in Figure 4-2, indicating the weaker peak on disk 2 became a local maximum which had the highest microwave energy concentration in the bottom half of the core. The added 2cm in height increased the surface area of the core, thus created "extra space" for the microwaves to penetrate from the side. The extra microwaves were absorbed and redistributed in the bottom half of the core such that a standing wave was formed around that area, with a peak on the 2nd disk manifested by the temperature. On the other hand, the 10.1cm diameter core reduced the microwave energies coming from the side significantly before they could reach the center, because its diameter is much larger than the microwave penetration depth. This led to the failure of forming standing waves at the bottom half of the core, and no peak was seen in the area.

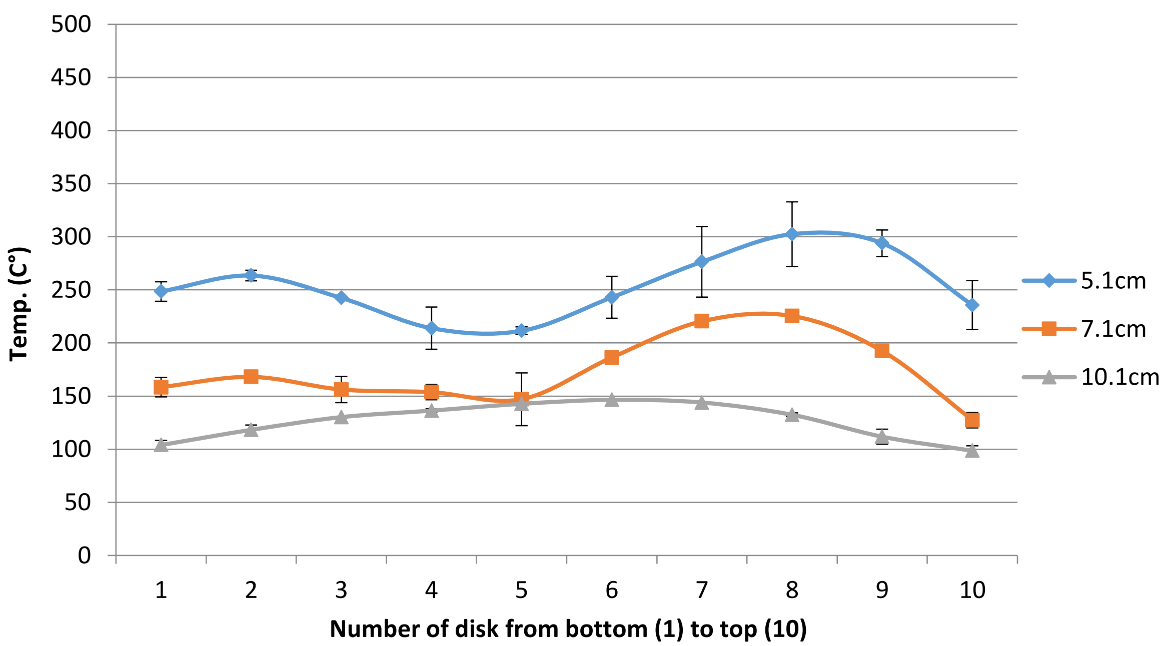

Figure 4-3. Temperature distributions of 10cm tall cores with three diameters

At 13 and 16cm heights, all cores had two temperature peaks located near the two ends (Figure 4-4 and 4-5), with a weaker peak in the bottom half and stronger peak in the top half of the cores. Again the unequal peaks were caused by the uneven electromagnetic energy distribution in the microwave oven. As noticed, the distances from the center of the core to the peaks were symmetrical, which were 4cm (disk 11- 7, and 7-3) for 5.1 and 7.1cm cores, and 3cm (disk 10-7, and 7-4) for 10.1cm cores, for the height of 13cm (Figure 4-4); and 5cm and 4cm for cores of 16cm height (Figure 4-5). Also in Figure 4-3, it is noticeable that the peaks in the 5.1 and 7.1cm cores were symmetrical about the center, and the distance was 3cm. It seemed as the height increased, both peaks tended to shift themselves away from the center symmetrically. However, the peaks also tended to shift away from the terminals of the cores. For 5.1 and 7.1cm cores, the weaker peak shifted from the 2nd disk to the 3rd disk when the height was changed from 10cm to 13cm (Figure 4-3 and 4-4), but remained in the same location when the height was changed from 13 to 16cm (Figure 4-4 and 4-5). On the other hand, the stronger peak remained in the same location from the top when the height was changed from 10 to 13cm (Figure 4-3 and 4-4), but shifted from the 11th to the 13th disk when height was changed from 13 to 16cm. For the 10.1cm core, the weaker peak shifted from the 4th to the 5th disk when the height was changed from 13 to 16cm, but the stronger peak remained in the same location from the top (Figure 4-4 and 4-5).

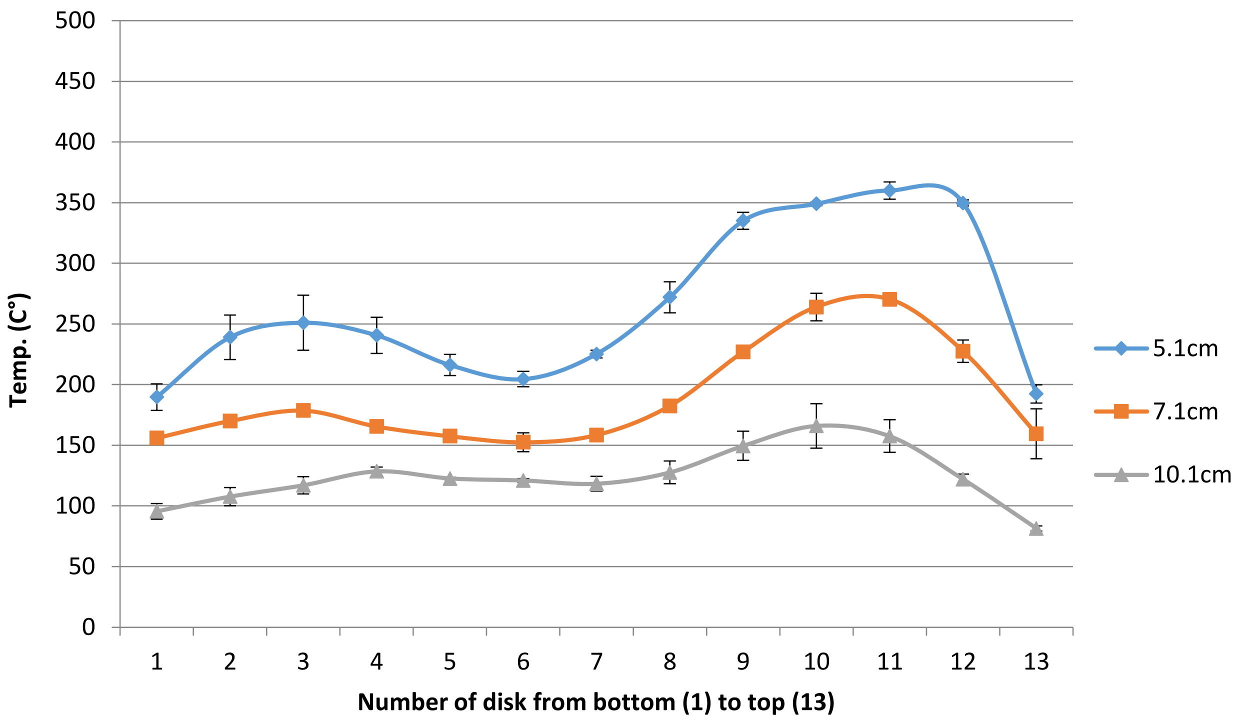

Figure 4-4. Temperature distributions of 13cm tall cores with three diameters

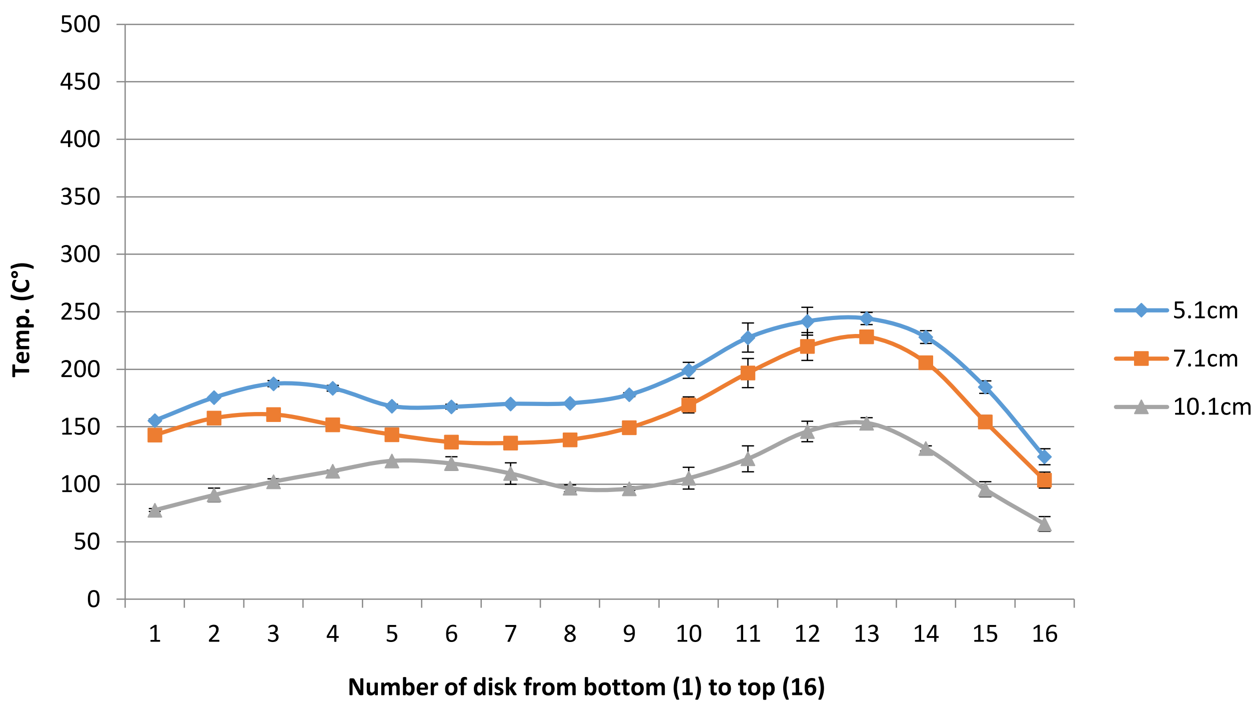

Figure 4-5. Temperature distributions of 16cm tall cores with three diameters

It is interesting to observe that when the height of the cylindrical core is small, the temperature peak is likely to be concentrated in the middle, whereas the temperature peaks are likely to be concentrated near the terminals in taller cores. Since the microwave radiation comes from every possible direction inside the cavity towards the core, standing waves are formed within the core in the sense that the peaks of the sanding waves are dependent on the diameter and height of the core. The diameter to height ratio for 5.1cm diameter cores to have two temperature peaks is $\frac{D}{H} = 0.5$; the ratio for the7.1cm diameter cores to have two temperature peaks is $\frac{D}{H} = 0.71$ and the ratio for the 10.1cm diameter cores to have two peaks is $\frac{D}{H} = 0.78$. These ratios are all smaller than one and increase as the diameter of the core increases. If the diameter to height ratio is equal or greater than 1, only one peak is seen in all the cores as in the case of 5cm high cores. Furthermore, if the diameter to height ratio can result in two peaks for the core that has the smallest diameter; it can also result in two peaks for cores with bigger diameters. For instance, the highest diameter to height ratio for the 5.1cm diameter cores to have two peaks is 0.5, which corresponds to 15cm height for the 7.1cm diameter core and 20cm height for the 10.1cm diameter cores. As shown in Figure 4-4, the 7.1cm diameter core with height of 16cm had two peaks and the 10.1cm diameter core with a height of 16cm also had two peaks, indicating two peaks are certainly to be expected for the 10.1cm core with a height of 20cm. As the height of a core increases, the two peaks tend to shift away from both the center and terminals, or in other words, towards the center of the top and bottom halves. It indicates that the temperature peak is formed such that it starts from the middle of the core. When the core reached certain height, the top and bottom halves were heated symmetrically as well as separately by microwaves coming from the side, and the weaker and stronger peaks were due to non-uniform energy concentration in the microwave oven. Microwaves coming from top and bottom may have influence on temperature distribution when the height of a core was low, but didn't play significant role in higher core, due to limited penetration depth.

In addition, the trend of temperature distribution for 10.1cm diameter core appeared to be smoother and more uniform than the 5.1 and 7.1cm cores, because the surface area of each disk in the 10.1cm diameter core is bigger, which makes it distribute heat more efficiently across itself than the 7.1cm diameter and 10.1cm diameter cores after receiving microwave treatment for the same amount of time.

4.2. Temperature distribution for cubed shaped cores

Because the thickness of each cubic of basalt is twice the cylindrical disk thickness, the locations of peaks for stacks of cube are expected to be at half the disk number, if they shall have the same pattern of temperature distribution. For 10cm (5 layer) stacks of cube with 4.5 width, the temperature peaks were located on the 1st and 4th disk (Figure 4-6), which is equivalent to peaks located on the 2nd and 8th disks of the 10 layer cylindrical cores with a diameter of 5.1cm (Figure 4-3). Similarly, for the 6cm wide stacks of cube, the temperature peaks were located on the 1st and 4th disk, whereas 9cm wide stack exhibited only one peak on the 3rd disk (Figure 4-6). For the 16cm (8 layer) stack of cubes with a diameter of 4.5cm, the temperature peaks were located on the 2nd and 6th disk from the bottom (Figure 4-7), which is equivalent to the peaks located on the 3rd and 12th disk of the 16 layer cylindrical core with diameter of 5.1cm (Figure 4-5). Similarly, the 6cm wide stack exhibited peaks on the 2nd and 7th disk and the 9cm wide stack exhibited peaks on the 2nd and 7th disk (Figure 4-7). In general, each cube in the core had a higher temperature than the equivalent cylindrical disk in a core; despite the fact the cores have the same trend of temperature distribution. This can be explained by Appendix 4: the thicker the disk, the more slowly the heat is transferred from a hotter to a colder disk. The 2cm thick cubes are more able to trap heat inside themselves instead of passing it to neighboring cubs.

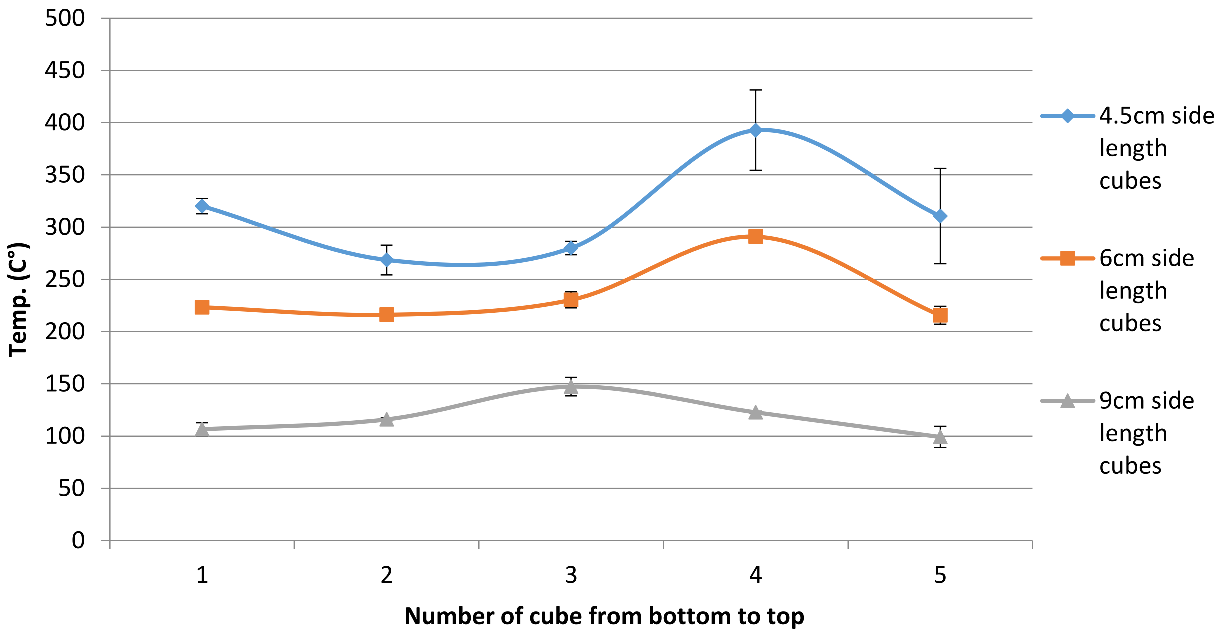

Figure 4-6. Temperature distribution of 8cm tall cores with three side lengths after microwave treatment for 90 sec

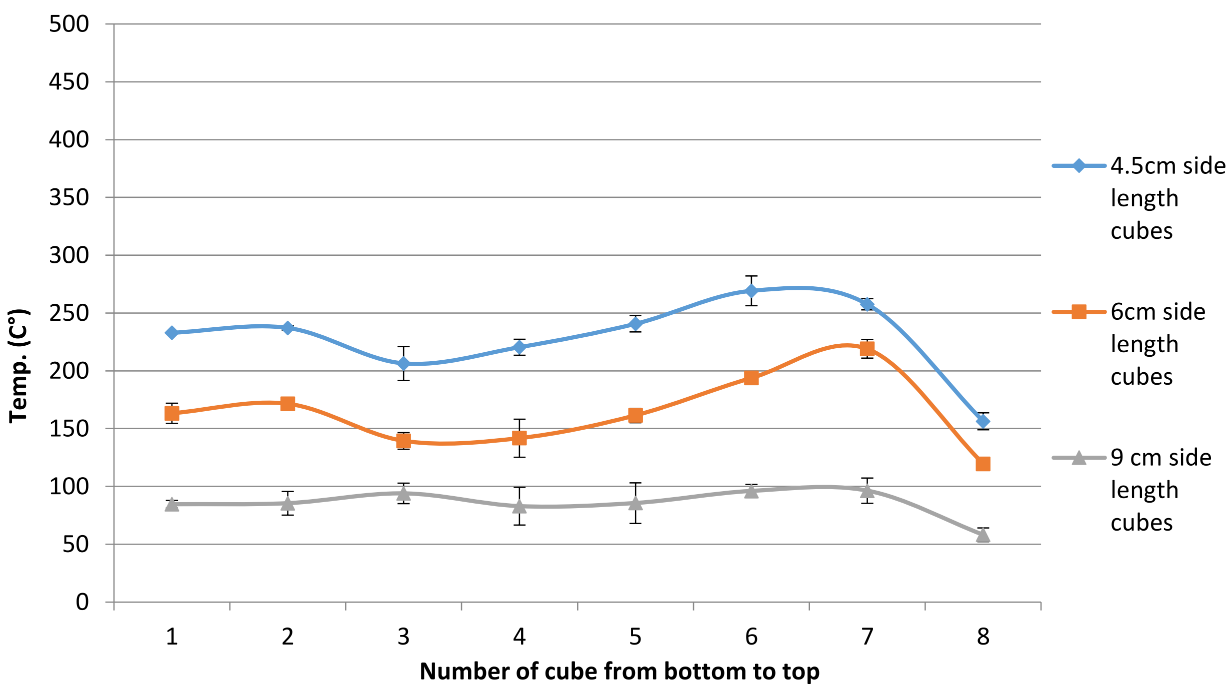

Figure 4-7. Temperature distribution of 16cm tall cores with three side lengths after microwave treatment for 90 sec

4.3. Influence of air spaces between disks in cylindrical cores on temperature distribution

Both cores that had 1mm spacing and had no spacing received microwave treatment for the same amount of time under the same condition. The results are shown from Figure 4-8 to 4-13.

At 90 sec (Figure 4-8), two peaks were seen in both trend lines, with one having stronger intensity at top half of the core and the other one with weaker intensity at bottom half of the core. The locations of the peaks were slightly different. The core having no spacing had peaks on the 2nd and 8th disk, whereas the core with spacing had peaks on the 3rd and 9th disk. As the heating time decreased, the difference of temperature distribution became less significant. At 60 sec (Figure 4-9), the two temperature trend lines looked almost similar to each other except for the locations of the peaks. At 30 and 20 sec (Figure 4-10 and 4-11), the two trend lines almost overlapped with each other. At 15 and10 sec (Figure 4-12 and 4-13), the temperature trend lines almost matched perfectly. The positive match in temperature distributions at all heating times indicates that spacing of 1mm in each layer of the 7.1cm cylindrical cores doesn’t have significant influence on the temperature distribution, especially at short heating times.

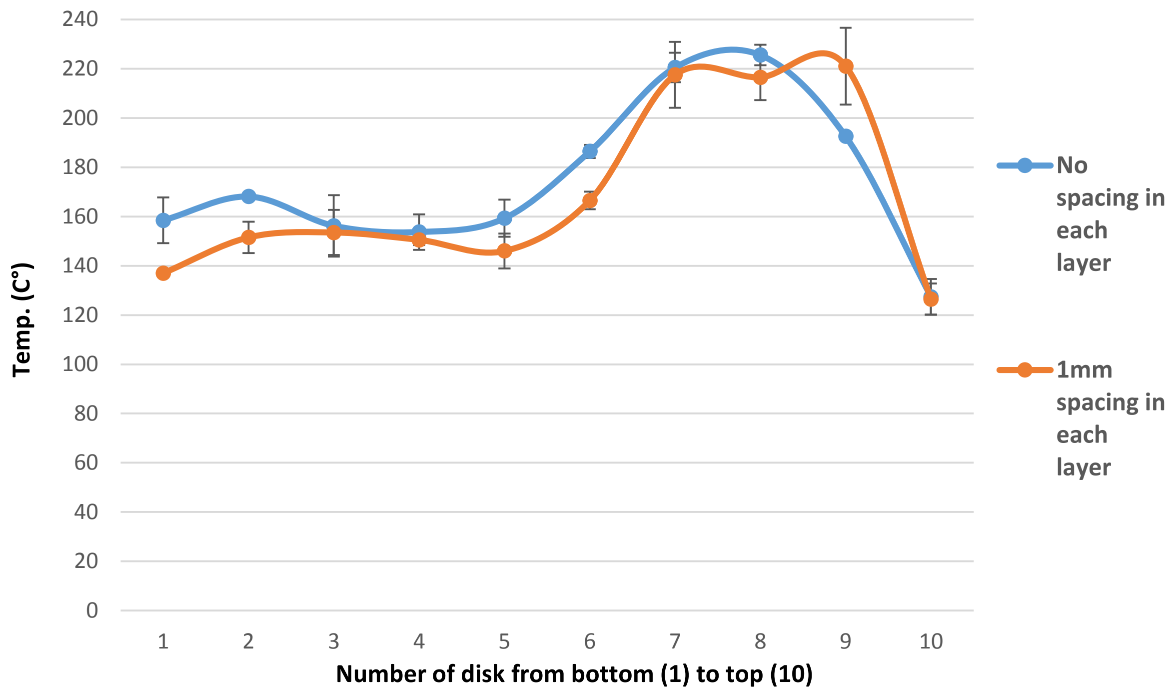

Figure 4-8. Temperature distributions of 10cm tall 7.1cm diameter cores with and without 1mm air space between each layer, after microwave treatment for 90 sec

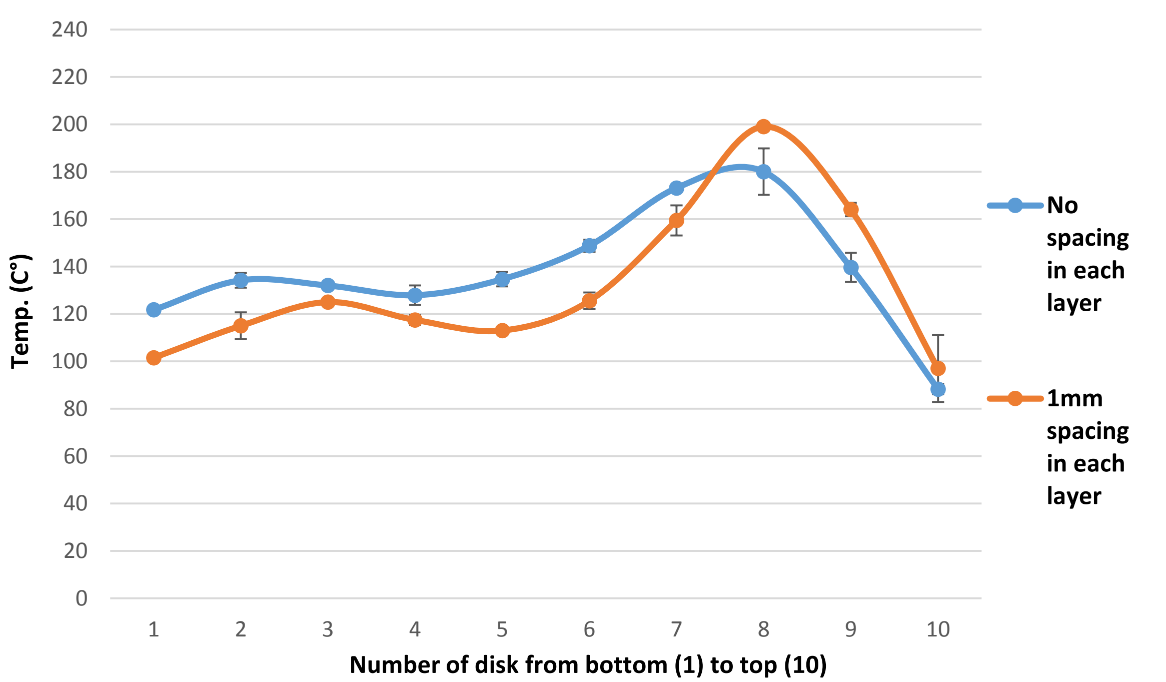

Figure 4-9. Temperature distributions of 10cm tall 7.1cm diameter cores with and without 1mm air space between each layer, after microwave treatment for 60 sec

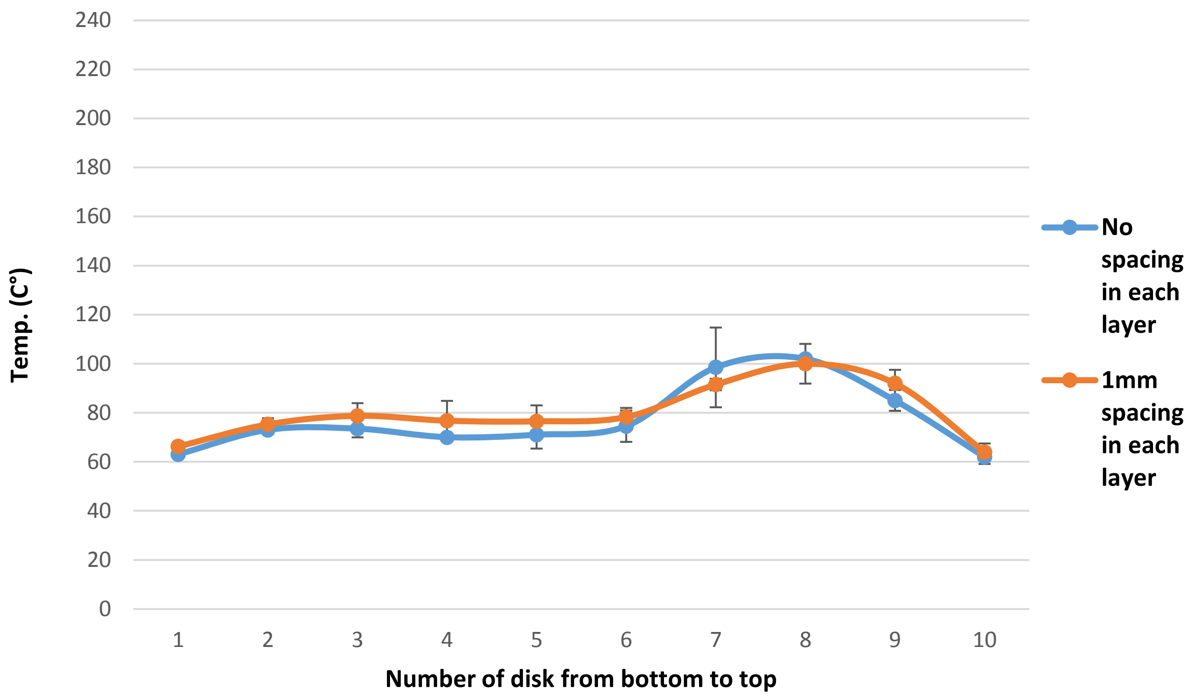

Figure 4-10. Temperature distributions of 10cm tall 7.1cm diameter cores with and without 1mm air space between each layer, after microwave treatment for 30 sec

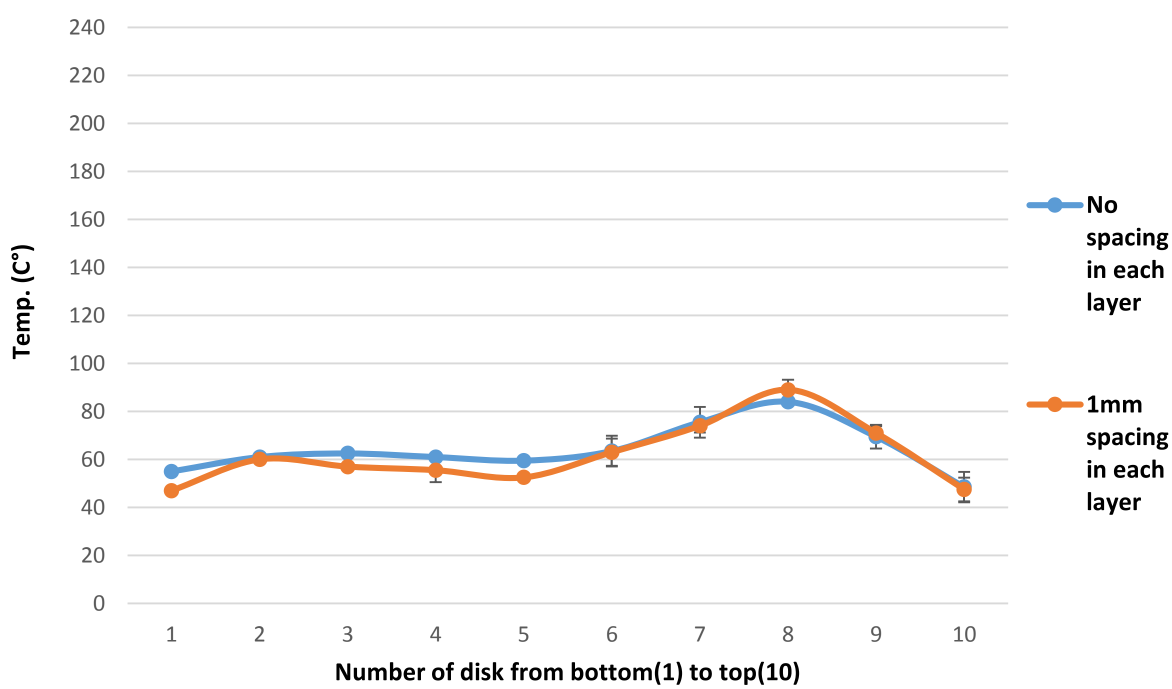

Figure 4-11. Temperature distributions of 10cm tall 7.1cm diameter cores with and without 1mm air space between each layer, after microwave treatment for 20 sec

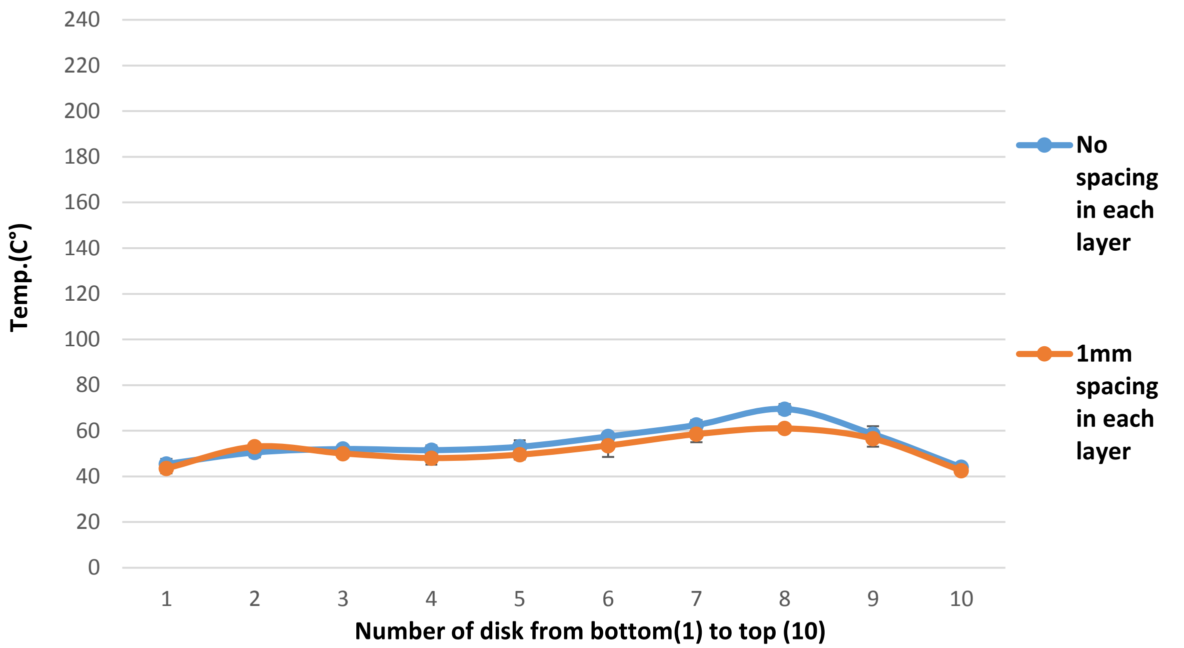

Figure 4-12. Temperature distributions of 10cm tall 7.1cm diameter cores with and without 1mm air space between each layer, after microwave treatment for 15 sec

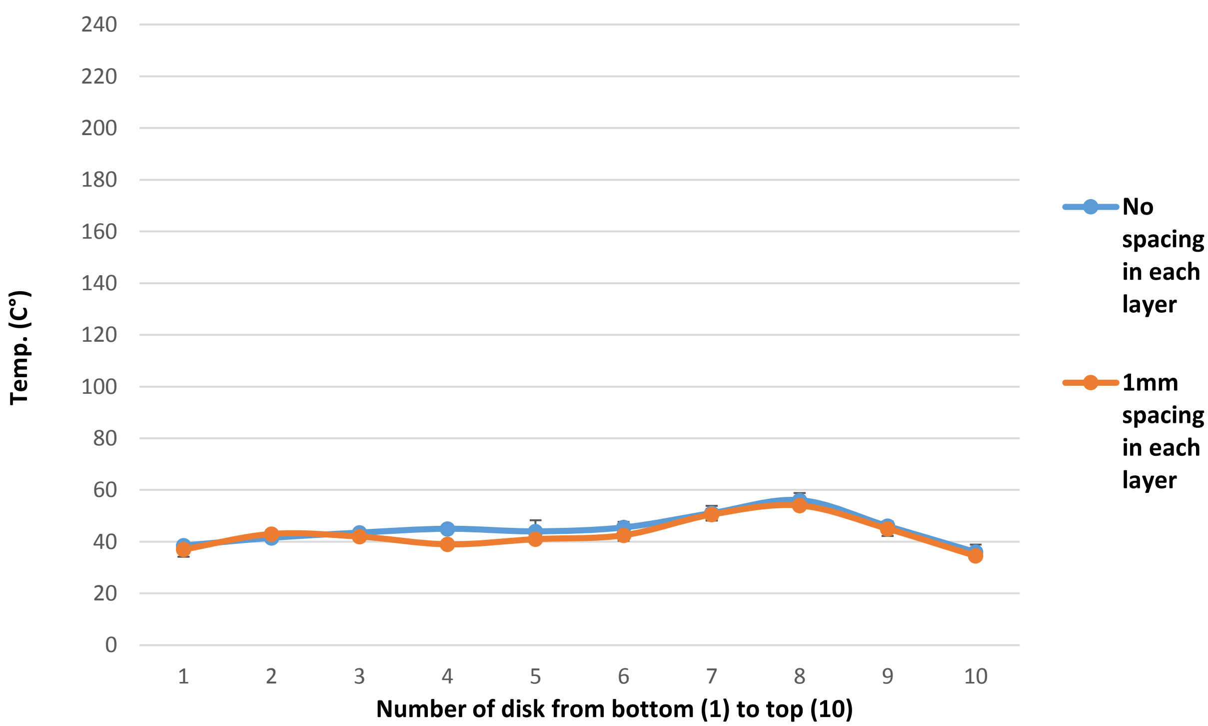

Figure 4-13. Temperature distributions of 10cm tall 7.1cm diameter cores with and without 1mm air space between each layer, after microwave treatment for 10 sec

The second test investigated the effect of air space size on the heating efficiency of microwaves using the setup introduced in Figure 3-9 and Figure 3-10. For convenience, the 5^{th} disk is the top disk and the 4^{th} disk the second disk. After microwave treatment for 30 or 60 sec, as the spacing between the top and second disk increased, the top disk tended to have a higher temperature, whereas the second disk tended to have a lower temperature.

When the top and second disks were in contact (0mm spacing), the temperature distributions for both 30 sec and 60 sec heating times are almost linear (grey lines in Figure 4-14 and 4-15). The pattern of distribution is independent of heating time. The temperature increased steadily from bottom to top disks. The discrepancy of temperature between the top and second disk is approximately 15 degrees for 30 sec and less than 20 degrees for 60 sec heating time.

When 1mm spacing was present between the top and second disk (yellow lines in Figure 4-14 and 4-15), the trends of temperature distributions became steeper but almost remained linear. The temperature difference between the first and second disk was 20 degrees for 30 sec and approximately 30 degrees for heating time of 60 sec.

As the spacing increased to 4mm (deep blue lines in Figure 4-14 and 4-15), the trend of temperature distributions of the cores stopped behaving linearly. A curve is clearer seen between the 3^{rd} and 5^{th} disk for cores at both heating times, an indication that temperature increased more rapidly in that area. The temperature difference between the top and second disk was approximately 30 degrees for 30 sec and 40 degrees for heating time of 60 sec. The bottom three disks (1-3) had almost the same temperatures at 30 sec.

As the spacing increased to 10mm (green lines in Figure 4-14 and 4-15), the temperatures in the top and second disk formed an intense curve, indicating that the temperature increased very rapidly from the second disk to the top disk. The temperature difference between the top and second disk was approximately 60 degrees for 30 sec and 100 degrees for heating time of 60 sec. It appeared that the top disk tended to absorb most of the energy after the spacing was significantly increased. For both heating times, the bottom four disks (1-4) had almost the same temperatures.

When the spacing further increased to 20mm (light blue lines in Figure 4-14 and 4-15), the temperatures of disks 1-4 were almost the same, regardless the heating time. The temperature of the top disk became significantly high and the difference between the top and second disk was approximately 90 degrees for 30 sec and 200 degrees for heating time of 60 sec. It appeared the top disk has absorbed almost the entire energy delivered to core.

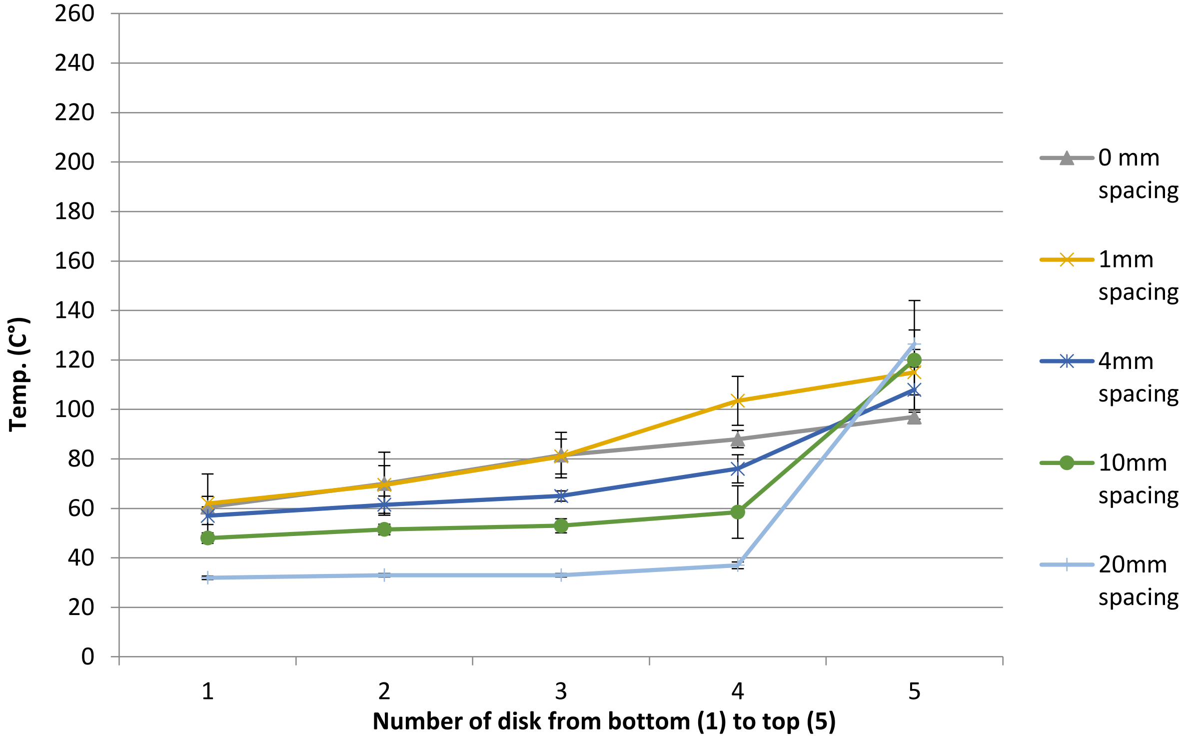

Figure 4-14. Temperature distributions of 5cm tall, 7.1cm diameter cores with different lengths of air spacing between the top and second disk microwaved for 30 sec

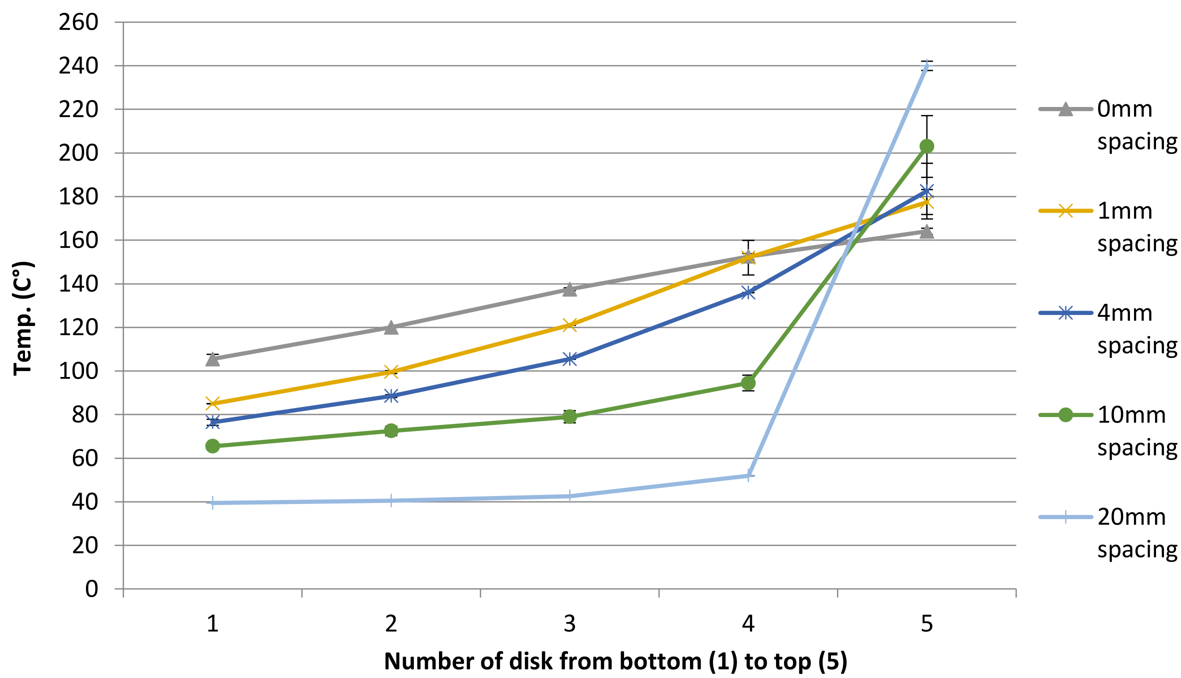

Figure 4-15. Temperature distributions of 5cm tall, 7.1cm diameter cores with different lengths of air spacing between the top and second disk microwaved for 60 sec

The percentage of temperature discrepancy $\frac{T_{top}-T_{second}}{T_{top}}$ between the top and second disk increased linearly with the increase of spacing after microwave treatment for 60 and 30 sec (Figure 4-19 and 4-20). At the spacing of 20mm, the percentage is almost 80%, compared to less than 10% when spacing was zero after microwave treatment of 60sec. The percentage of difference is more than 70% at 20mm spacing, compared to 10% when spacing was zero, for 30sec of microwave treatment. The slope is 0.0351 and the correlation factor is 0.98 for 60 sec heating time; and 0.0316 and 0.95 for 30 sec. The high correlation factors indicate that by increasing the spacing to beyond 20mm, the percentage of temperature discrepancy between the top and second disk will most likely follow a linearly fashion and increase with a steady rate.

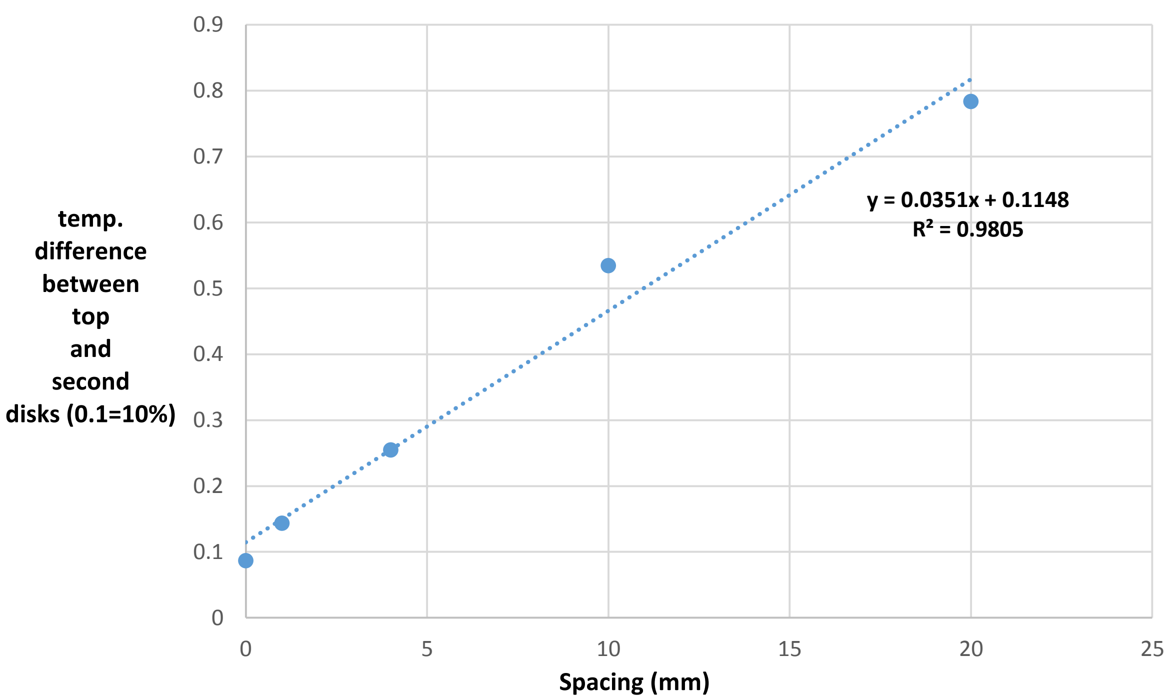

Figure 4-16. Linear regression between percentage of temperature difference between the top and second disk and the size of the air space in cylindrical stacks on basalt microwaved for 60 sec

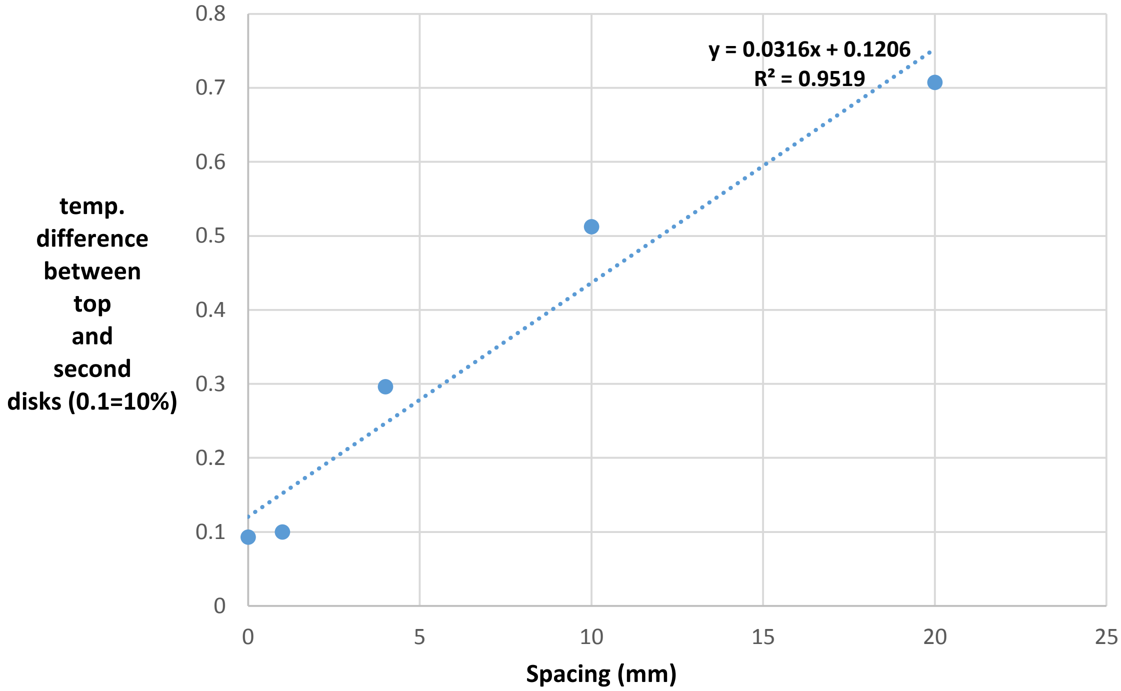

Figure 4-17. Linear regression between percentage of temperature difference between the top and second disk and the size of the air space in cylindrical stacks on basalt microwaved for 30 sec

The cause of the temperature discrepancy either comes from the limited amount of microwave energy that can reach the second disk when spacing increases or the decreases of convection rate when spacing is large. Given the microwave penetration depth of 4cm, and the reflection coefficient of approximately 50% between the basalt and air (Appendix 2), microwaves lose about 70% of their energy when they reach the second disk after leaving the top disk (Figure 4-21). Since air is an almost lossless medium to microwaves, they dissipate very little energy to the air while travelling in the space. The amount of microwave energy that can reach the second disk from the top is always the same, as long as there is spacing, even if the spacing is very tiny, because the loss factor of air is almost zero. The temperature discrepancy between the top and second disk should be independent with spacing. However, the experimental results in Figure 4-19 and 4-20 show a linear dependence of temperature discrepancy on spacing. This is attributed to convection by the air trapped in the space, which plays a dominant role in transferring the heat from the hotter disk to the colder disk. When the spacing is not present, the microwaves don't lose much energy when they reach the second disk. The temperature discrepancy is less than that shown in Figure 4-19 and 4-20, which is approximately 10%. When the spacing is very small (i.e., 1mm) microwaves lose 70% of energy via travelling in different mediums before they reach the second disk, but since the spacing is small enough, the air molecules trapped inside are in frequent contact with each other, which facilitates the heat transfer. Therefore the temperature discrepancy is approximately10-15%, depending on the heating time.

As the spacing increases to 4mm, the amount of microwave energy that can reach the second disk doesn't change significantly, but the air molecules are in less contact with each other, which leads to less efficient heat transfer and a temperature discrepancy approximately 30%. As the spacing further increases to 10mm, the air starts to become less efficient in conducting heat due to even less molecular activity, and the temperature discrepancy increases to 50%. When the spacing is 20mm, the air starts to serve as an insulator of heat; therefore the disk at the top is not able to transfer much heat to the second disk but rather absorbs almost all the microwave energy, the second disk can only absorb approximately 30% of the energy that the top disk absorbs without getting much from the air, which results in a temperature discrepancy approximately70-80%.

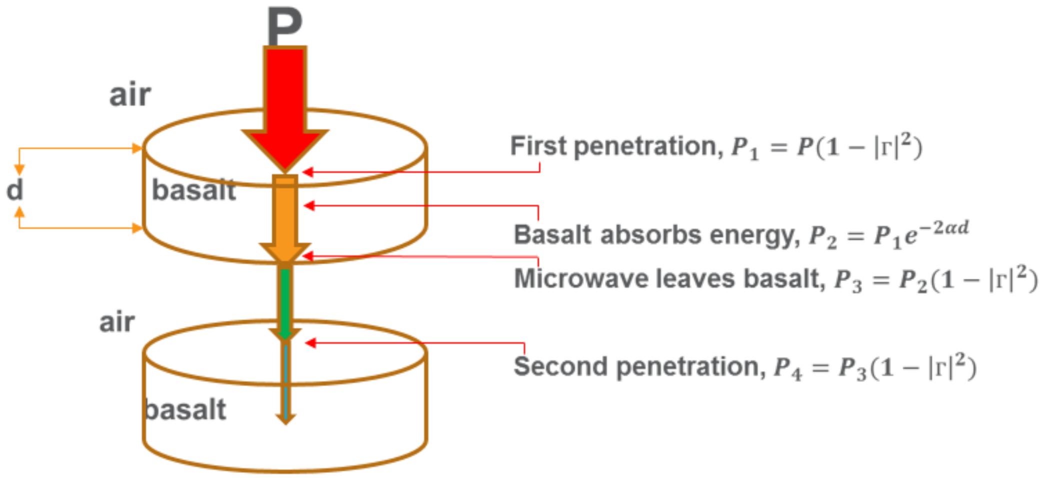

$$P_4 = Pe^{-2\alpha d}(1-|\Gamma|^2)^3$$

$$\frac{P_4}{P} = e^{-2\alpha d}(1-|\Gamma|^2)^3 = e^{-2\cdot 12.5\cdot 0.01}(1-0.25)^3 = 0.32$$

Figure 4-18. Schematic view of microwave energy losing energy via reflection and penetration

4.4. Relationships between power absorption and cylinder volume and temperature

The power absorbed by the entire cylinder increased with cylinder volume, with the best fit trend line having a power function (Figure 4-22). Therefore, the rate of increase slowed at larger volumes. Figure 4-22 also predicts that by increasing the volume, the power absorption will most likely follow a trend line given by a power series.

It is interesting to see that by omitting the middle term of equation 2.2(3), which is reminded here:

$$P = \frac{T-T_0}{t}\rho C V = \omega \varepsilon_0 \varepsilon''_{eff} E^2_{rms} V \qquad 2.2(3)$$

The following equation can be obtained:

$$P = \omega\varepsilon_0\varepsilon''_{eff}E^2_{rms}V \quad 4.1(1)$$

Equation 4.1(1) would be a perfect linear function with the volume V as the independent variable (input), the power absorption P as dependent variable (output) and $\boldsymbol{\omega\varepsilon_0\varepsilon''_{eff}E^2_{rms}}$ as the slope, if the value of $\boldsymbol{E^2_{rms}}$ is constant everywhere inside the core. All the data in Figure 4-22 would perfectly land on the trend line. However, in reality $\boldsymbol{E^2_{rms}}$ reduces fast as microwaves penetrate into the cores, therefore an ideal linear correlation between the volume and power absorption doesn't exist. The best way to establish a relationship between the power absorption of the core and volume is by providing data obtained through empirical measurement, in which case high accuracy is difficult to achieve, rather only a general correlation can be obtained.

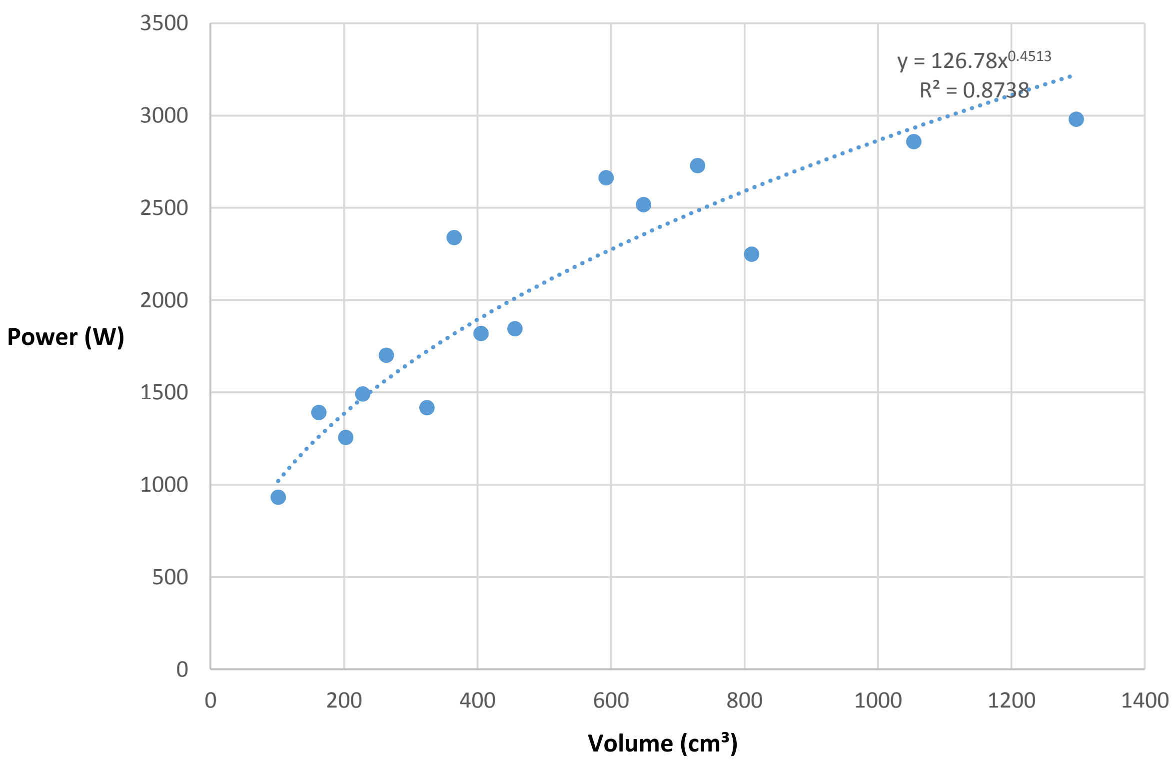

Figure 4-19. Power relationship between power absorbed by cylindrical cores and cylinder volumes

Despite the fact that the power absorption increases with volume, the temperature on the other hand, decreases with increased volume (Figure 4-23) and the trend of decreasing followed a power series of decreasing order. It is also interesting to realize that by ignoring the term on the left part in equation 2.2(3), the following can be obtained:

$$\frac{T-T_0}{t}\rho CV = \omega\varepsilon_0\varepsilon''_{eff}E^2_{rms}V \qquad 4.1(2)$$

The Volume V on both sides of equation 4.1(2) can cancel each other if the square of RMS electric field E^2_{rms} is the same everywhere across the core. If this is the case, the temperature would be independent on volume but solely on the electric field as indicated in equation 4.1(3):

$$\frac{T-T_0}{t}\rho C = \omega\varepsilon_0\varepsilon''_{eff}E^2_{rms} \qquad 4.1(3)$$

However, this theoretical model completely excluded the relationship between temperature and volume, which is not true in reality, again due to the fact that E^2_{rms} is not constant. Therefore only the empirical method can be used to establish the correlation between the temperature and volume in which case enough data will be needed to find the best fit regression trend line.

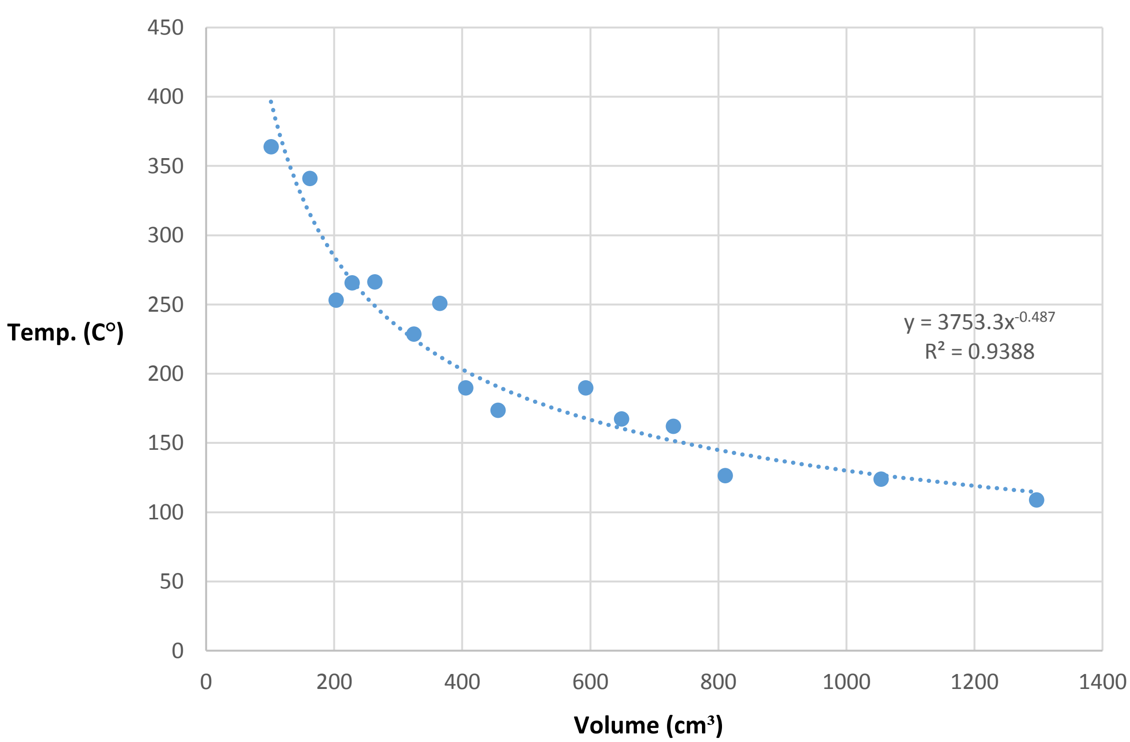

Figure 4-20. Correlation between temperature and volume after microwave treatmement

V. Conclusions and discussion

When a multimode microwave cavity is empty the energy distribution is chaotic, caused by individual waves bouncing off the conducting walls to form standing waves that have nodes and anti-nodes on all dimensions. When a high loss object is placed in the cavity it rapidly absorbs microwaves coming from all dimensions. The distribution of electromagnetic energy inside the object results in various energy concentrations in different location, reflected by temperature profile. According to the temperature profile of 5.1, 7.1 and 10.1cm diameter cores of different heights after microwave treatment, the following can be concluded.

1. For the same height, the smallest diameter core always had the highest temperature
2. Two peak temperatures located near the ends of the core were observed in the cores with diameter to height ratios of 0.5, 0.7, and 0.78. The rate of increase in peak temperature slowed with increasing ratio. At ratios greater than 1, only one peak temperature was observed.
3. When only one peak was present, the peak shifted towards the top of the core with increment of height due to higher energy concentration in the top half of the microwave oven
4. When two peaks were present, the peaks tended to shift towards the center of the top and bottom halves of the core symmetrically with the increment of height
5. Microwaves coming from the top and bottom of the core had little effects on temperature distribution when the height was large due to limited penetration depth
6. Conduction helped transfer heat between disks; core with larger diameter had smoother and more uniform temperature distribution

The temperature distribution for cubic shaped and cylindrical shaped cores were close to each other, indicating the shapes of the cores don't differentiate the temperature distributions from one to another as long as they have the same volume. Despite the fact both cylindrical and cubic cores have the same temperature distribution; the average temperature of individual disks in the cubic core is higher than the ones in the cubic cores. This can be explained by conduction theory listed in Appendix 4.

The effect of an air space increased with spacing size and microwave treatment time. At heating time less than 30 sec, the two temperature distributions were similar, which indicates that in am multimode cavity, where the microwave radiation comes from every direction, the tiny spacing in a regular shaped object such as cylinder has little influence on the temperature distribution.

Increasing spacing affected the temperature distribution in the cores exposed to plane microwaves. The temperature difference between the top disk directly exposed to the microwave radiation and the second disk which "hid" underneath it linearly increased with spacing for 30 and 60 sec microwave treatments. This observation was not due to a decrease in the amount of microwave energy that could reach the 2nd disk, because air is not a good absorber of microwave energy. Rather, the convection played a significant role when the spacing was small and was insignificant when the spacing was large.

Regression method was used to estimate the correlation between the power absorption and volume, and between temperature and volume of the cylindrical cores. 15 sets of data known as volume were chosen as input (independent) variables through which 15 sets of output data known as were calculated using equation 2.2(3). The power absorbed increased with volume increase following a power series with R^2 of 0.87, indicating the volume increase of a cylinder can help absorb more energy, but the rate of absorption slows in larger volumes. The theoretical model presented in equation 4.1(1) couldn't be used because the electric field is not constant in the cores. On the other hand, 15 sets of data known as temperature were chosen as dependent variable to establish a correlation with volume. Results have shown the temperature decreased with volume following a power series of decreasing order with $R^2$of 0.94, indicating that larger volume would result in lower average temperature in the core, but the rate of temperature decrease slows down at larger volumes.

The increase of energy absorbed and decrease of temperature with volume increase indicate that high energy absorption doesn't necessarily result in high temperature everywhere across the core, rather heating non-uniformities will generate a few high and low temp spots across in the core as described from Figure 4-1 to 4-5. The non-uniformity is so tremendous that the overall temperature decrease with increase of power absorption.

The errors introduced in the experiments include the assumption that all factors that can influence the permittivity remained the same during the heating process. Disks were not treated and measured simultaneously. Any delay between treatment and measurement allowed disks to lose heat to the surrounding air; In addition, small variations in disk shape and surface smoothness after cutting and grinding were introduced to equipment limitations and human errors. Only the central temperature in each disk was measured and extrapolated to represent the disk's overall temperature. In fact, temperatures differ between the center and periphery because of the penetration depth of microwave. An intact core was assumed to behave the same as the a core created by stacking individual disks. Conduction plays an important and complex role in temperature distribution, and was not directly measured. Simulation software would be a good tool to calculate temperature distribution for an intact core.

VI. References

1. **A.C. Metaxas and R.J. Meredith**, “Industrial microwave heating”, Peter Peregrinus Ltd, London, United Kingdom,1983
2. **Aleksander Prokopenko**, “Microwave Heating for Emolliating and Fracture of Rocks, Advances in Induction and Microwave Heating of Mineral and Organic Materials”, Prof. StanisÅ‚aw Grundas (Ed.), ISBN: 978-953-307-522-8
3. **B. B. S. Singhal, R. P. Gupta**, “Applied Hydrogeology of Fractured Rocks*”,* DOI 10.1007/978-90-481-8799-7_2, © Springer Science+Business Media B.V. 2010
4. **BENGTSSON, N. E., and RISMAN, P. D,** “Dielectric properties of foods at 3 GHz as determined by a cavity perturbation technique. II. Measurements in food materials”, J. *Microwave Power* 6(2), 107 (1971)
5. **Bernhard Maidl, Leonh Schmid, Willy Ritz, Martin Herrenknecht and David S. Sturge**, “Hard rock tunnel boring machines”, 2008, ISBN 978-3-433-01676-3
6. **C. A. Pickles**, “Microwaves in Extractive Metallurgy: A Review of Fundamentals**”**, DOI: 10.1016/j.mineng.2009.02.015
7. **D.A. Jones, S.W. Kingman, D.N. Whittles *, I.S. Lowndes**, “Understanding microwave assisted breakage”, 2004
8. **David K. Cheng**, “Field and Wave Electromagnetics”, Syracuse University, Addison-Wesly, 2004, ISBN: 0201528207, 9780201528206
9. **David M. Pozar**, “Microwave Engineering”, Wiley; 4 edition (Nov. 22 2011), ISBN: 978-0470631553

10. **Docfrankie.com**

11. **Fawwaz T. Ulaby, Tom Bengal, M. Craig Dobson, Jack East, Jim Garvin, and Diane Evans**, "Microwave dielectric properties of dry rocks", IEEE, August 2002

12. **Ferri Hassani, Pejman Nekoovaght**, "THE DEVELOPMENT OF MICROWAVE ASSISTED MACHINERIES TO BREAK HARD ROCKS**",** 2011 Proceedings of the 28th ISARC, Seoul, Korea

13. **FRED HAPGOOD**, "The Underground Cutting Edge: The innovators who made digging tunnels high-tech Invention & Technology v.20, n.2", Fall 2004

14. **G.R. Olhoeft**, "Electrical Properties of Rocks" 1976

15. **Hartman, Howard L.**, "SME Mining Engineering Handbook", Society for Mining, Metallurgy, and Exploration Inc., 1992, p3

16. **HARVEY, A. F**.,"Microwave Engineering, Academic Press, New York (1963)

17. **Hashizume & Ebara & Yusa Lab**, "http://afre.qse.tohoku.ac.jp/webmaster@karma.qse.tohoku.ac.jp. Copyright ©"

18. **Hasted, J.B.,** "Aqueous Dielectrics", Chapman and Hall, London (1973)

19. **Hogan, C. Lester (1953)**, "The Ferromagnetic Faraday Effect at Microwave Frequencies and its Applications", Reviews of Modern Physics **25** (1): 253-262, doi: 10.1103/RevModPhys.25.253

20. http://mainland.cctt.org/istf2008/generators.asp

21. **Huang, J.H., Rowson, N.A.**, "Hydrometallurgical decomposition of pyrite and marcasite in a microwave field" June 2002, Pages 169–179, DOI: 10.1016/S0304-386X(02)00041-5

22. **J.C. Maxwell**, "A Treatise on Electricity and Magnetism",1873

23. **JAMES, C. R., TINGA, W., and VOSS, W. A. G**., "Energy Conversion in Closed Microwave Cavities", Microwave Power Engineering (Edited by E. C. Okress), Vol. 2, pp. 28-37.Academic Press, New York (1968).

24. **James R. Wang and Thomas J. Schmugge** "an Empirical Model for Complex Dielectric Permittivity of Soils as a Function of water content" IEEE, April 23, 2007, ISSN: 0196-2892

25. **J. de los Santos; D. Garcia; J.A. Eiras**, "Dielectric characterization of materials at microwave frequency range", Feb 2003, Materials Research, vol.6 no.1

26. **John W. Walkiewicz, Andrea E. Clark, and Sandra L. McGill**, "Microwave-Assisted Grinding" IEEE, 06 August 2002, ISSN 0093-9994

27. **Kazi E. Haque**, "Microwave energy for mineral treatment processes—a brief review", International Journal of Mineral Processing, Volume 57, issue 1, July 1999, Page 1-24

28. **Kingman S.W., Vorster W., Rowson N.A.**, (2000), "The effect of microwave radiation on the processing of Palabora Copper ore", JSAIMM., vol 100, No 3, May/June 2000, pp 197 – 204.

29. **Mark N. Wuddivira, David A. Robinson, Inma Lebron, Laëtitia Bréchet, Melissa Atwell, Michael Oatham , Scott B. Jones, Hiruy Abdu, Aditya K. Verma, Markus Tuller**, "Estimation of Soil Clay Content fromHygroscopic Water Content Measurements", 2012, Soil Sci.Soc.Am.J., doi: 10.2136/sssaj2012.0034

30. **McGill S.L., Walkiewicz J.W. & Smyres G.A.**, "The effects of power level on the microwave heating of selected chemicals and minerals", Proc. Materials Res. Soc. Symp. Microwave Processing Materials, Vol. 124, pp. 247-253. Reno, 1988

31. **Michael Coulson**, “The History of Mining: The events, technology and people involved in the industry that forged the modern world”, Harriman House Limited, 12 November 2012

32. **Michael W. Davidson,** “Electromagnetic Radiation, Interactive Java Tutorials”, 1998

33. **MUDGETT, R. E., MUDGETT, D. R., GOLDBLITH, S. A., WANG, D. I. C, and Westphall,W. B**., “Dielectric properties of frozen meats”, J. Microwave Power 14(3), 209 (1979)

34. **National Research Council (U.S.)**, Committee on Microwave Processing of Materials: An Emerging Industrial Technology, National Materials Advisory Board, Commission on Engineering and Technical Systems, (1994). Microwave processing of materials. Washington D.C.: National Academy Press.

35. **N. Standish, W. Huang**, “Microwave application in carbothermic reduction of iron ore”, ISIJ Int. 31 (1991) 241–245

36. **N. Yoshikawa, E. Ishizuka, K. Mashiko, S. Taniguchi**, “Carbon reduction kinetics of NiO by microwave heating of the separated electric and magnetic fields”, Metall. Mater, Trans. B 38 (2007) 863–868 on Industry Appl., 1991, Vol. 27, No. 2, pp. 239-243

37. **Pejman Nekoovaght Motlagh**, “An investigation on the influence of microwave energy on basic mechanical properties of rocks”, Master thesis, 2009

38. **R.K. Amankwah , G. Ofori-Sarpong**, “Microwave heating of gold ores for enhanced grindability and cyanide amenability”, Mineral Engineering, Volume 24, Issue 6, May 2011, Page 641-644

39. **Richard.C.DORF, Editor-in-Chief, 2003,** “The electric engineering handbook,” 2nd edition, ISBN 0-8493-1586-7

40. **Roberts. S and Von Hippel**, A.R., "J Appl. Phys. 17, 610",1946

41. **Rzepecka, M.**, "A cavity perturbation method of routine permittivity measurements", J microwave power 8(1), 3(1973)

42. **Sir. Russel Madigan**, "Of Minerals and Man", 1981, ISBN: 0909520607, 9780909520601

43. **S.M. Javad Koleini and Kianoush Barani**, "Microwave Heating Applications in Mineral Processing", "The development and application of microwave heating, chapter 4", November 7, 2012

44. **S.W. Kingman, K. Jackson, S.M. Bradshaw, N.A. Rowson, R. Greenwood**, "An investigation into the influence of microwave treatment on mineral ore comminution", Powder Technology Volume 146, Issue 3, 8 September 2004, Pages 176–184

45. **STUCHLY, S. S., and HAMID, M. A. K.,** "Physical parameters in microwave heating processes", J. Microwave Power 7(2), 117 (1972).

46. **Tathamay Basu, Kartik K. Iyer, Kiran Singh* & E. V. Sampathkumaran**, "Novel dielectric anomalies due to spin-chains above and below N$\acute{e}$el temperature in $Ca_3Co_2O_6$", scientific reports, October 31, 2013

47. **Tim Napier-Munn, Barry A. Wills**. "Wills' Mineral Processing Technology: An Introduction to the Practical Aspects of Ore Treatment and Mineral Recovery", August 2006, ISBN: 978-0-7506-4450-1

48. **Tinga, W.**, "Multiphase dielectric theory applied to cellulose mixtures", PhD Thesis, Universityof Alberta, Edmonton, Canada (1969)

49. **Warren L.Stutzman, Gary A. Thiele**, “Antenna theory and design”, 2nd Edition, 1998. ISBN 978-0-471-02590-0

50. **WINDLE, J. J., and SHAW, T. M.,** “Dielectric properties of wool-water mixtures”,J. *Chem.Phys.* 22,1752 (1954).

51. **William H. Hayt, Jr.John A. Buck**, “Engineering Electromagnetics”, McGraw-Hill Science/Engineering/Math; 8th edition (Jan. 28 2011), ISBN-10: 0073380660, ISBN-13: 978-0073380667

52. **Yanmin Wang and Eric Forssberg**, “International overview and outlook on comminution technology”, Föreningen Mineralteknisk Forskning / Swedish Mineral Processing Research Association, 2003

Appendices

Appendix 1

The reflection coefficient between basalt and air is:

$$\Gamma = \frac{\eta_{air}-\eta_{basalt}}{\eta_{air}+\eta_{baslat}} = \frac{\sqrt{\frac{\mu_0}{\varepsilon_0}}-\sqrt{\frac{\mu_0\mu_{basalt}}{\varepsilon_0\varepsilon_{baslat}}}}{\sqrt{\frac{\mu_0}{\varepsilon_0}}+\sqrt{\frac{\mu_0\mu_{basalt}}{\varepsilon_0\varepsilon_{baslat}}}} = \frac{377-377\frac{1}{\sqrt{8.6-j1.35}}}{377+377\frac{1}{\sqrt{8.6-j1.35}}} = \frac{249-j10}{504+j10} =$$

$$0.49 + j0.029 = 0.49\angle 3.4^o$$

$|\Gamma| = 0.5.$ It indicates that the magnitude of reflected microwave is half of the incident wave and the portion of energy transmitted to either side from basalt or air is

1-$|\Gamma|^2 = 1 - 0.25 = 0.75$, indicating 75% of the energy can be transmitted from basalt to air or vice versa.

Appendix 2

The penetration depth of basalt is

$$D_p = \frac{1}{2\alpha} = \frac{1}{2\omega}\frac{\sqrt{2}}{\sqrt{\mu_0\varepsilon_0}\sqrt{\mu_0\varepsilon'}}\frac{1}{\sqrt{\sqrt{1+(\frac{\varepsilon''_{eff}}{\varepsilon'})^2-1}}} = \frac{\sqrt{2}}{2}\frac{\lambda_0}{2\pi}\frac{1}{\sqrt{8.6}}\frac{1}{\sqrt{\sqrt{1+(\frac{1.35}{8.6})^2-1}}} =$$

$$\frac{0.17}{12.57\times\sqrt{8.7-8.6}} = \frac{0.17}{4.1} = 0.04m$$

λ_0 is the microwave wavelength in free space which is 12.2cm. Therefore

$\alpha = \frac{1}{2 \cdot 0.04} = 12.5$NP/m, NP stands for nepers, which is a unit to describe the magnitude drop of an electromagnetic wave per meter.

Appendix 3

Even though it is not intuitive and difficult to analyze refraction problems with cylindrical disks because of their curved boundary, modifications can be made by unfolding the disk along its tangent so that it becomes a square, indicated on the left graph below. Therefore the problem has been switched to the analysis of refraction effects for cubic disks, indicated on the fight graph below.

When microwave is penetrating at a random angle θ_3 to the normal direction indicated by the blue line from one side of basalt sample, the refracted angle is θ_2. The microwave keeps travelling inside the sample until it hits the surface that is perpendicular to the one from which it penetrates into, and then the second refraction occurs, this time from a denser medium (basalt) to a looser medium (air). The incident angle now is θ_4 and the refracted angle is θ_5. According to Snell's law, during the first refraction:

$$\frac{\sin \boldsymbol{\theta_3}}{\sin \boldsymbol{\theta_2}} = \frac{\boldsymbol{n_{bal}}}{\boldsymbol{n_{air}}} = \frac{\boldsymbol{k_{bal}}}{\boldsymbol{k_{air}}} \qquad \text{A1}$$

And during the second refraction:

$$\frac{\sin \boldsymbol{\theta_4}}{\sin \boldsymbol{\theta_5}} = \frac{\boldsymbol{n_{air}}}{\boldsymbol{n_{bal}}} = \frac{\boldsymbol{k_{air}}}{\boldsymbol{k_{bal}}} \qquad \text{A2}$$

The relationship between $\boldsymbol{\theta_4}$ and $\boldsymbol{\theta_1}$ is $\boldsymbol{\theta_4} = 90^o - \boldsymbol{\theta_1}$, and therefore

$$\sin \boldsymbol{\theta_4} = \cos \boldsymbol{\theta_1} = \sqrt{1 - (\sin \boldsymbol{\theta_1})^2} \qquad \text{A3}$$

According to the geometry of the graph,

$$\sin\boldsymbol{\theta_1} = \frac{b}{d} \tag{A4}$$

And

$$\sin\boldsymbol{\theta_2} = \frac{a}{d} \tag{A5}$$

Therefore

$$\sin\boldsymbol{\theta_1} = \frac{b}{a}\sin\boldsymbol{\theta_2} \tag{A6}$$

Plug the above equation to A3:

$$\sin\boldsymbol{\theta_4} = \sqrt{1-(\frac{b}{a}\sin\boldsymbol{\theta_2})^2} \tag{A7}$$

Plug the above equation to A2:

$$\frac{\sqrt{1-(\frac{b}{a}\sin\boldsymbol{\theta_2})^2}}{\sin\boldsymbol{\theta_5}} = \frac{\boldsymbol{n_{air}}}{\boldsymbol{n_{bal}}} = \frac{\boldsymbol{k_{air}}}{\boldsymbol{k_{bal}}} \tag{A8}$$

And rearrange the above equation:

$$\sin\boldsymbol{\theta_2} = \frac{a}{b}\sqrt{1-(\frac{\boldsymbol{k_{air}}}{\boldsymbol{k_{bal}}}\sin\boldsymbol{\theta_5})^2} \tag{A9}$$

Plug the above equation in A1:

$$\sin\boldsymbol{\theta_3} = \frac{\boldsymbol{k_{bal}}}{\boldsymbol{k_{air}}}\frac{a}{b}\sqrt{1-(\frac{\boldsymbol{k_{air}}}{\boldsymbol{k_{bal}}}\sin\boldsymbol{\theta_5})^2} \tag{A10}$$

Since

$$\boldsymbol{k} = \boldsymbol{Im}\{\boldsymbol{jK}\} = \boldsymbol{\omega}\sqrt{\frac{\mu\varepsilon'}{2}}(\sqrt{\mathbf{1}+\left(\frac{\varepsilon''}{\varepsilon'}\right)^{\mathbf{2}}}+\mathbf{1})^{\frac{1}{2}} \tag{A11}$$

And the dielectric constant and loss factor for air and basalt are 1 and 0, and 8.6 and 1.35, the frequency of microwave is 2.45GHz, and the dielectric permeability for both basalt and air is 1, plug these numbers into equation A11, therefore:

$$\boldsymbol{k_{air} = Im\{jK_{air}\} = 2\pi \times 2.45 \times \sqrt{\frac{1}{2}}(\sqrt{1+\left(\frac{0}{1}\right)^2}+1)^{\frac{1}{2}}} \qquad \text{A12}$$

And

$$\boldsymbol{k_{bal} = Im\{jK_{bal}\} = 2\pi \times 2.45 \times \sqrt{\frac{1\times 8.6}{2}}(\sqrt{1+\left(\frac{1.35}{8.6}\right)^2}+1)^{\frac{1}{2}}} \qquad \text{A13}$$

Therefore

$$\boldsymbol{\frac{k_{bal}}{k_{air}} = \frac{2.94}{1}} \qquad \text{A14}$$

and

$$\boldsymbol{\frac{k_{air}}{k_{bal}} = \frac{1}{2.94}} \qquad \text{A15}$$

Plug A14 and A15 back to A10, it is easy to get:

$$\boldsymbol{\sin\theta_3} = 2.94\ \frac{a}{b}\sqrt{1-(\frac{1}{2.94}\boldsymbol{\sin\theta_5})^2} \qquad \text{A16}$$

Since $a \geq b$ all the time according to the geometry, $\frac{a}{b} \geq 1$ all the time

Plug $\frac{a}{b} \geq 1$ in A16 and rearrange A16; it is not difficult to get:

$$(\boldsymbol{\sin\theta_5})^2 \geq 8.64 - (\boldsymbol{\sin\theta_3})^2 \qquad \text{A17}$$

When $\boldsymbol{\sin\theta_3} = 1$

$$\boldsymbol{\sin\theta_5} \geq 2.76 \qquad \text{A18}$$

A17 and A18 indicate that even when the microwave is penetrating from the side wall with an angle of 90 degrees to the normal direction, or more specifically, grazing the side wall without penetration, the angle at which it leaves the surface that is perpendicular to the side wall is bigger than 90 degrees. Since the angle at which the microwave leaves the basalt increases as the angle at which the microwave penetrates into the basalt decreases according to A17, total reflection always occurs regardless at which angle the microwave penetrates from the side wall of the basalt.

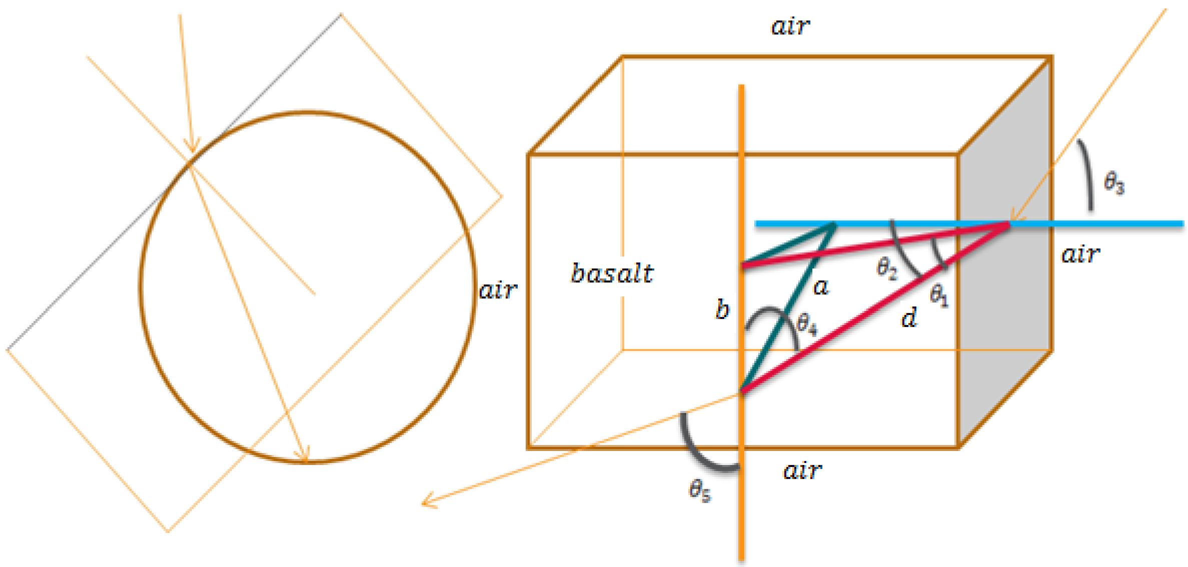

Appendix 4

The rate of thermal transfer through conduction is:

$$\frac{Q}{t} = \frac{\kappa A(T_{hot} - T_{cold})}{d}$$

κ is the conductivity, A is the surface area, d is the thickness on the direction of heat flow, and T_{hot} and T_{cold} are the temperatures of hot and cold areas of an object. The equation indicates the rate of thermal or heat transfer $\frac{Q}{t}$ is proportional to the object's surface area and inversely proportional to its thickness. Convection, on the other hand, doesn't have as much impact in dissipating heat from the object to air therefore in this part of the experiment we have ignored its influence.